~~A well-constrained, coccolith-specific~~A clumped isotope calibration of ~~cultured coccolithophorids~~coccoliths at well-constrained culture temperatures for marine temperature reconstructions

Alexander J. Clark[1], Ismael Torres-Romero[1], Madalina Jaggi[1], Stefano M. Bernasconi[1], and Heather M. Stoll[1]

[1]Department of Earth Sciences, ETH Zürich, Switzerland

Correspondence to: Alexander J. Clark (aclark@ethz.ch)

Abstract. Numerous recent studies have tested the clumped isotope (Δ_{47}) thermometer on a variety of biogenic carbonates such as foraminifera and bivalves and showed that most follow a common calibration. However, there may be a difference between biogenic carbonate-based calibrations and the most recent inorganic carbonate calibrations that are assumed to have formed close to isotopic equilibrium. Biogenic calibrations such as those based on foraminifera from seafloor sediments suffer from uncertainties in the determination of the calcification temperatures. Therefore, well-constrained laboratory cultures without temperature uncertainty can help resolve these discrepancies. Although the sample size requirements for a reliable Δ_{47} measurement have decreased over the years, the availability and preservation of many biogenic carbonates is still limited and/or require substantial time to be extracted from sediments in sufficient amounts. Coccoliths, on the other hand, are abundant and often well-preserved in sediments, and are a potential interesting target for palaeoceanography. We thus determined the Δ_{47}-temperature relationship for coccoliths ~~because they are relatively easy~~due to ~~grow~~their relative ease of growth in the laboratory. The carbon and oxygen isotopic compositions of coccolith calcite have limited use in palaeoenvironmental reconstructions due to physiological effects that cause variability in the carbon and oxygen isotopic fractionation during mineralisation. However, the relatively limited data available suggest that clumped isotopes may not be significantly influenced by these effects. We cultured three species of coccolithophores under controlled carbonate system conditions with $CO_{2(aq)}$ concentrations between 5 and 45 μM, pH between 7.9 and 8.6 units, and temperatures between 6°C and 27°C.

Our well-constrained results agree with a previous culture study that there are no apparent species- or genus-specific vital effects on the Δ_{47}-temperature relationship in coccolithophores despite significant deviations from equilibrium in the C and O isotopic composition. We find that varying environmental parameters other than temperature does not have a significant effect on Δ_{47}, changing the parameters yields coccolith Δ_{47}-temperature calibrations that agree within 1.2 ppm. Our ~~well-constrained~~ coccolith-specific Δ_{47}-temperature calibration with well-constrained temperatures shows a consistent, positive offset of 2-3°C to the inorganic carbonate calibrations, which point to as yet unknown coccolith-specific disequilibrium effects. ~~All published biogenic studies fall within within ±1°C of our coccolith-specific calibration if the original calcification temperatures are~~

considered, while a cold bias and offsets of 1-2°C are present using the recalculated calcification temperatures of a recent study.

Thus, we suggest the use of our coccolith-specific calibration for further coccolith palaeoceanographic studies and that calibrations derived from laboratory-grown biogenic carbonates, in particular foraminifera, are desirable to reinforce the
35 confidence of clumped isotope-based temperature reconstructions in palaeoceanography.

1 Introduction

Clumped isotope thermometry is a relatively new and increasinglyan increasing commonly used methodology for the reconstruction of paleotemperatures, palaeohydrology, diagenetic regimes, and as an isotopic tracer (see Huntington and Petersen, 2023 for a recent review). In a carbonate molecule, bonds between the rare heavy isotopes ^{13}C and ^{18}O can be formed
40 and their excess abundance relative to a stochastic distribution is denominated as "clumping", which increases with decreasing temperature. To measure this clumping, the carbonate is converted to CO_2 by reaction with phosphoric acid, and the excess abundance of $^{13}C^{18}O^{16}O$ (cardinal mass 47) in the released CO_2 relative to a stochastic distribution is measured and reported as Δ_{47} (Schauble et al., 2006; Eiler, 2007). In early studies, before the introduction of carbonate standardisation (Bernasconi et al. 2021), Δ_{47} in different calibration studies of the same carbonate material had widely variable relationships with temperature.
45 More recent studies (Petersen et al., 2019; Meinicke et al., 2020; Anderson et al., 2021) have shown that most but not all of these discrepancies were caused by poor interlaboratory comparability caused by the lack of a robust standardisation methodology (Bernasconi et al. 2018, 2021).

Based on these recent studies, Δ_{47} has a consistent relationship with temperature and its temperature dependence is well established empirically at a large range of temperatures (e.g., Anderson et al., 2021; Fiebig et al., 2021). The Δ_{47}-temperature
50 relationship is independent of the carbon and oxygen isotope composition of the fluid from which carbonates precipitate (Ghosh et al., 2006). Empirical calibrations between temperature and Δ_{47} have been established for temperatures between 0°C and 1100°C for inorganic carbonates (Kele et al., 2015; Bonifacie et al., 2017; Kelson et al., 2017; Müller et al., 2019; Swart et al. 2019; Jautzy et al. 2020; Anderson et al., 2021). Further empirical studies on biogenic carbonates, such as for foraminifera, coccoliths, gastropods, and bivalves, have found similar relationships between Δ_{47} and calcification temperature
55 (Katz et al., 2017; Peral et al., 2018; Leutert et al., 2019; Piasecki et al., 2019; de Winter et al., 2022; Huyghe et al., 2022), although specific types of biogenic carbonates such as shallow-water corals (Spooner et al., 2016; Davies et al., 2022), juvenile bivalves (Huyghe et al., 2022), and brachiopods (Bajnai et al., 2018; Davies et al., 2023; Letulle et al., 2023) do not. However, there are clear discrepancies between on the one hand most inorganic calibrations (Swart et al. 2019; Jautzy et al. 2020; Anderson et al., 2021; Fiebig et al., 2021) and an often used, generalised biogenic calibration (Meinicke et al., 2020). One
60 interpretation is that this discrepancy results from uncertainties in the calculation of calcification temperatures for planktonic foraminifera and is resolved with an alternate approach to calcification temperature estimation (Daëron and Gray, 2023). With

this study using cultured coccoliths, we generate biogenic carbonate under well-constrained temperature conditions, so there is very little uncertainty in the calcification temperatures.

Other methodological problems can also limit the overall use of clumped isotopes. The relative abundance of Δ_{47} to all isotopologues of CO_2 is only ~45 ppm, which requires a sample in the range of 80 to 120 µg with Thermo-Fischer Kiel IV devices coupled to Thermo-Fischer 253 Plus mass spectrometers (Müller et al., 2017) to 2-10 mg for a single measurement with common acid bath systems (e.g. Ghosh et al., 2006; Kelson et al., 2017; Peral et al., 2018; Fiebig et al., 2021). As the analytical error in clumped isotope measurements is large compared to the natural variability, many replicates are needed to achieve an analytical uncertainty allowing meaningful interpretations in palaeoceanography (Bernasconi et al., 2021; Fernandez et al., 2017; Daëron, 2021). Sample size requirements can be a major limiting factor for biogenic calcite. Both limited abundance and time requirements for picking single species, limits the availability of planktonic foraminifera, and the need for sampling precise seasonal increments in slow-growing molluscs can also restrict the mass of carbonate available for analysis (Leutert et al., 2019; de Winter et al., 2022; Huyghe et al., 2022). Coccoliths are a promising alternative as they are often found in greater abundance and have a better preservation potential than foraminifera (Berger, 1973; Subhas et al., 2019).

The abundance of coccolith-associated-polysaccharides (CAPs) both around and within the coccolith aid in protecting the coccolith calcite from dissolution and overgrowth, and remain in place for millions of years (Henriksen et al., 2004; Sand et al., 2014; Lee et al., 2016). FewIn part due to these CAPs, coccolithophores have a fine control on the formation of coccolith calcite. Calcite crystals are nucleated in a circular protococcolith ring upon an organic baseplate within the coccolith vesicle, which subsequently matures into a coccolith (Brownlee et al., 2015; Walker et al., 2019). The coccolith is then extruded towards the exterior of the cell, where it is adhered to the cell and forms an interlocking system of coccoliths known as a coccosphere (Brownlee et al., 2015; Taylor et al., 2017; Walker et al., 2018). CAPs and other organic compounds are found in abundance in all calcification steps. Intracrystalline CAPs from different species of coccolithophores can be crystal-inhibiting (such as for *E. huxleyi*; Henriksen et al., 2004; Gal et al., 2016; Walker et al., 2019) or promote calcite specifically even in unfavourable conditions (such as for *G. oceanica*; Walker et al., 2019). Extracrystalline CAPs can aid in adherence of the coccolith to the cell, of the coccoliths to each other, and maintain the coccosphere structure (Walker et al., 2018). Subsequently, there are few anion substitutions and a lack of lattice defects on the coccolith surface that further aid in a better preservation relative to foraminifera (Berman et al., 1993; Stoll et al., 2001; Frøhlich et al., 2015; Walker et al., 2019). Additionally, there are a multitude of specialised pathways that regulate the fluxes of cations such as Ca^{2+} and dissolved inorganic carbon (DIC) species into various intracellular compartments to allow for controlled calcification and photosynthesis (Brownlee et al., 2015; Gal et al., 2017; Taylor et al., 2017).

Biogenic carbonates often feature carbon and oxygen isotopic compositions that differ from those expected for abiogenic carbonates near equilibrium, offsets informally called "vital effects"., as a result of the complexity of coccolith calcification described above. Such offsets have been described for coccolith calcite (Ziveri et al., 2003; Rickaby et al., 2010; Ziveri et al., 2012; Candelier et al., 2013; Hermoso et al., 2014; Stevenson et al., 2014; Hermoso et al., 2016, Katz et al., 2017) and the contributing processes simulated in models (Langer et al., 2012; Ziveri et al., 2012; Bolton and Stoll, 2013; Holtz et al., 2017;

McClelland et al., 2017). The vital effects limit the use of stable isotope signatures of coccolith calcite in palaeoceanography. However, initial studies of clumped isotopes in coccolithophorids found that while multiple coccolithophore species display clear carbon and oxygen vital effects, they follow previous Δ_{47}-temperature calibrations (Drury and John, 2016; Katz et al., 2017), making them potentially useful for palaeoceanography. However, because these studies and calibrations were

100 performed before carbonate standardisation (Bernasconi et al., 2021) and have a limited number of replicate analyses, robustness and interpretation of their conclusions need to be verified with new studies. Other aspects such as the dissolved inorganic carbon chemistry in the cultures and growth conditions as possible influences on Δ_{47} also still need to be examined. To this end, three species of calcifying coccolithophores were cultured under controlled temperature and carbonate chemistry conditions. A temperature range of 21°C and $CO_{2(aq)}$ range of 40 μM was covered. Coccolithophores from the *Gephyrocapsa*

105 genus were cultured between 6°C and 27°C, using the warm-adapted *G. oceanica* and the cold-adapted *G. muellerae*. Inter-genus vital effects were tested through comparison with *Calcidiscus leptoporus*, which features distinct carbon and oxygen isotopic vital effects compared to *Gephyrocapsa* in previous studies (Ziveri et al., 2003; Hermoso et al., 2014; Katz et al., 2017). Finally, through comparison with a previous coccolith culture (Katz et al., 2017), inorganic (Anderson et al., 2021; Daëron and Vermeesch, 2024), biogenic (Peral et al., 2018; Meinicke et al., 2020; de Winter et al., 2022), and recalculated

110 (Daëron and Gray, 2023) Δ_{47}-temperature calibrations, the potential need for a coccolith-specific calibration is assessed.

2 Materials and methods

2.1 Batch and continuous culture setup

Three monoclonal coccolithophore strains, *Gephyrocapsa oceanica* (RCC 1303), *Gephyrocapsa muellerae* (RCC 3370), and *Calcidiscus leptoporus* (RCC 1130) obtained from the Roscoff Culture Collection were cultured at ETH Zürich. *G. oceanica*

115 is an abundant cosmopolitan coccolithophore species that has been found at temperatures between 12-27°C but favours temperatures above 20°C (Sett et al., 2014; von Dassow et al., 2021). *G. muellerae* is from the same genus as *G. oceanica*, favours colder and less saline conditions, and can grow at 6°C (von Dassow et al., 2021). *C. leptoporus* is a large coccolithophore, is especially abundant in low latitude upwelling settings, is resistant to dissolution and thus a major contributor to coccolith carbonate, and is known to have large isotopic vital effects (Thierstein and Young, 2004; Ziveri et al.,

120 2007; Langer et al., 2012; Hermoso, 2014). Thus, the three strains were cultured to provide a temperature range of 21°C while also highlighting potential isotopic vital effects. *G. oceanica* was cultured in a turbidostat or continuous culture setup as seen in Fig. 1a, between a $CO_{2(aq)}$ of 5 and 45 μM for at least two temperatures (Table 1). All three strains were grown in at least two temperatures in batch culture setup as seen in Fig. 1b, and provide a wide range of temperatures (Table 1).

All cultures were carried out in artificial seawater, following Kester et al. (1967), as the basis of a K/2 medium (Keller et al.,

125 1987). The final pH and DIC were adjusted through addition of HCl and Na_2CO_3 and covered a range of 40 μM of $CO_{2(aq)}$

values. A Tris buffer was not included for all experiments as this would interfere with the carbonate chemistry control. Prior to inoculation, the K/2 media was sterilized through an 0.2 µm Millipore Stericup filter.

Before starting the experiments, the strains were maintained at a constant temperature of 18°C and slowly acclimatized to the experimental temperature for at least 4-6 generations. Cultures were inoculated at cell densities of ~5000 cells mL^{-1} for *G. oceanica* and *G. muellerae* and ~2000 cells mL^{-1} for *C. leptoporus*.

Batch cultures were carried out in 1 or 2 L Nalgene polycarbonate sterile flasks with 50- and 100-mL headspace respectively and kept in a lit incubator set to the experimental temperature (± 0.1°C). For the duration of the experiments, the flasks were rotated on a roller set at 10 rpm to reduce settling and allow for uniform light exposure, see Fig. 1b. *C. leptoporus* did not grow under turbulent conditions and was manually shaken every day (Houdan et al., 2006). The cultures were illuminated by LED lights on a sinusoidal 14/10-hour light/dark cycle and a maximum luminosity of 120 µmol photons m^{-2} s^{-1}. Harvesting took place in a semi-continuous manner, where 80-90% of the total volume was harvested and then refreshed when the culture reached a set cell density (100-150 x 10^3 cells mL^{-1}). In general, we used a higher cell density compared to previous culturing studies due to the larger sample material requirement for clumped isotope measurements. Yet each strain was maintained in their early- to mid-exponential phase to prevent a reservoir effect and an enriching of the $\delta^{13}C$ of the media ($\delta^{13}C_{DIC}$) relative to the initial conditions (Barry et al., 2012; Hermoso, 2014). Certain batch and continuous cultures had a higher cell density and significant drift in the DIC, pH, or $CO_{2(aq)}$ over the course of the experiment and serve to test the sensitivity of vital effects to a varying carbon system.

Continuous cultures were performed in 1L (FMT 150/1000) or 3L (FMT 150/3000) photobioreactor (PBR) connected to a PP600 peristaltic pump and a GMS 150 gas mixing system (Photon Systems Instruments, Drásov, Czech Republic), see Fig. 1a. For a more detailed description of the experimental setup see Zhang et al. (2022). The strains were illuminated with LEDs on a 16/8-hour light/dark cycle with a maximum luminosity of 200 µmol photons m^{-2}s^1. The optical density (OD), which is proportional to the cell density, was calibrated to a zero point before inoculation. With continuous OD monitoring and (sub-)daily measurements of the cell density, the OD could be set to a cell density threshold between 100 and 200 x 10^3 cells mL^{-1}. If the OD exceeded this threshold, the peristaltic pump pumped fresh media into the PBR equivalent to 10% of the culture volume, and media from inside the PBR was pushed into the outflow bottle. Ambient air was first scrubbed of CO_2 and then passed through a gas mixing system with a set amount of CO_2 with a constant composition ($\delta^{13}C$ = -14.36 ± 0.06‰ VPDB; $\delta^{18}O$ = 19.85 ± 0.14‰ VSMOW). Thus, the pCO$_2$ was controlled and maintained at a constant level, which was checked at the beginning and end of each experiment. Temperatures were continuously controlled with a pH-temperature probe in the vessel, which kept a constant temperature with <0.1°C deviation through Peltier-elements at the bottom of the vessel.

Cell density and size were measured using a Z2 Coulter Particle Counter and Size Analyzer with an aperture size of 100 µm (Beckman Coulter, Inc., Brea, California, United States), which were used to determine growth rates. Cell counts were taken systematically every 24 hours with an extra measurement taken before and after harvest.

The net growth rate for batch cultures were calculated as:

$$\mu = \frac{\ln(N_t) - \ln(N_0)}{t - t_0} \tag{1}$$

where N_t is the cell count at time t (in days) and N_0 is the initial cell count.

For continuous cultures, the dilution rate, which equates to the volume of the output (V_{out}) over the volume of the PBR over time t also needs to be considered:

$$\mu = \frac{\ln(N_t) - \ln(N_0) + \frac{V_{out}}{V_{PBR}}}{t - t_0} \tag{2}$$

Cells were harvested by centrifugation at 4000 rpm for 5 minutes. The pellet containing coccoliths was rinsed with deionized water to remove traces of salts by 4 cycles of centrifugation and removal of the supernatant. Subsequently, the wet pellet of organic matter and coccoliths was transferred to a 2 mL vial, which was then stored at -20°C for later analysis.

At the beginning, at each harvest, and at the end of an experiment, 12 mL of water were sampled for pH and cell density measurement. Each aliquot was centrifuged once at 4000 rpm for 5 minutes, and the supernatant was used for DIC, $\delta^{13}C_{DIC}$, and $\delta^{18}O_{SW}$ measurements. Some batch and continuous cultures were kept until higher cell densities were reached. In these cases, pH, DIC, and $\delta^{13}C_{DIC}$ were measured more often to track the evolutions from initial conditions as a result of cell growth and cell density increase.

2.2 Sample cleaning

Contaminants from organic matter or sulphur compounds contained within carbonates are known to interfere with the clumped isotopic measurements for carbonates (Eiler and Schauble, 2004; Dennis and Schrag, 2010). In this study we used three methodologies for the removal of possible contaminants from the coccolith pellet. Initially the aliquots were dried in a 60°C oven for at least 4 hours to remove any remaining water that could dilute the cleaning reagents. Then one of three cleaning methodologies was performed.

One method used oxidation of the organic matter through reaction with a 18% H_2O_2 solution neutralized with NaOH to pH 8-9 following the protocol of Falster et al. (2018). The second methodology used a solution of 10% H_2O_2 neutralized with NH_3 to pH 8-9. For both solutions the pellets were reacted overnight at room temperature and then rinsed 4-5 times with milli-Q until a neutral pH of 7 was obtained. The third method used is Total Lipid Extraction (TLE), following Matyash et al. (2008). The pellets were first suspended in 1 mL of isopropanol and homogenized through vortexing and sonication until there were no visible clumps. 3 mL of methyl-tert-butyl ether were added and the total solution was again vortexed. 1 mL of DI water was added and the sample was centrifuged at 4000 rpm for 5 minutes. This method removes the polar and apolar organic compounds from the pellet into the upper 4 mL of the solution. This supernatant is subsequently discarded, while maintaining a 1 mL of aqueous phase with the cleaned coccolith pellet at the bottom. When abundant organic matter was still visible after one cycle of cleaning, the procedure was repeated. After all three cleaning methodologies, the samples were dried at 60°C for at least 4 hours.

In order to confirm the effectiveness of the different cleaning methodologies and their effect on the coccolith carbonate, high resolution scanning electron images were taken using a JSM-7100F JEOL Scanning electron Microscope (SEM) at ScopeM, ETH Zürich, see Fig. S1. As harvested from the cultures, all coccoliths exhibited regular morphology with no evidence of coccolith malformation. The cleaning protocol causes slight dissolution, fragmentation, and breakage of some of the coccoliths. Any difference in isotope measurements as a result of cleaning protocols was within the standard deviation or error of each measurement (± 0.15‰ for $\delta^{13}C$ and $\delta^{18}O$; ± 0.016 for Δ_{47}).

2.3 Isotope measurements

2.3.1 Coccolith carbon, oxygen, and clumped isotopes

Carbon, oxygen, and clumped isotopes from the cultured coccoliths were measured on two ThermoFisher Scientific mass spectrometers, a MAT253 and a 253Plus, coupled to Kiel IV preparation devices as described in Müller et al. (2017). Aliquots of 110-180 µg of sample and carbonate standards (ETH-1, 2, 3, and IAEA C2) were measured with a Kiel device at 70°C. The samples were reacted for 300 seconds with three drops of 104% phosphoric acid, and the released CO_2 was immediately frozen in a liquid nitrogen (LN_2) trap kept at -190°C. After the sample was reacted fully, the first LN_2 trap is heated to -100°C, and the CO_2 gas was transferred through a 10 mm PorapakQ (50-80 mesh) to a second LN_2 trap kept at -190°C. The PorapakQ tubing was coated with Sulfinert 2000, stuffed with silver wool, and kept at -40°C to capture and eliminate possible organic contaminants. The second LN_2 trap was then heated to room temperature and measured using the Long Integration Dual Inlet protocol (Hu et al., 2014, Müller et al., 2017). The initial gas intensity of the sample gas is recorded and then immediately measured for 400 seconds, 40 cycles of 10 seconds. Subsequently, the reference gas is measured for the same duration starting at the same initial gas intensity. Before measuring, background scans at different beam intensities were carried out to determine the pressure dependent background on all beams (Bernasconi et al., 2013; Meckler et al., 2014). Using the Easotope software (John and Bowen, 2016) a pressure-sensitive baseline correction was applied, and raw carbon and oxygen values were converted to VPDB using the Brand parameters as suggested by Daëron et al. (2016). Further, the raw vs accepted Δ_{47} values for the carbonate standards and an empirical transfer function were used to convert and normalize the sample Δ_{47} data to the Intercarb carbon dioxide equilibrium scale (I-CDES; Bernasconi et al., 2021).

Each individual reported clumped isotope value consists of at least 10 replicates, with an average of 13 replicates. Long-term accuracy and reproducibility of the Δ_{47} measurements were evaluated based on monitoring of the IAEA-C2 international carbonate standard, which was treated as an unknown sample (MAT253: $\Delta_{47} = 0.6385 \pm 0.034$, MAT253 Plus: $\Delta_{47} = 0.6411 \pm 0.026$‰; 1σ n=241) and fit within the accepted values (0.6409‰ $\pm$ 0.003‰; Bernasconi et al., 2021). Analytical errors are reported at the 95% confidence interval (Fernandez et al., 2017) without taking into account the standardisation error. However, as the measurements are carried out with a 50:50 standard to sample ratio, the additional uncertainty related to standardisation would be small (Bernasconi et al. 2021).

2.3.2 DIC and seawater carbon and oxygen isotopes

DIC and pCO_2 were measured on a Picarro G-2131-i Cavity Ringdown Spectrometer (Picarro Inc, USA) coupled to a AS-D1 DIC-$\delta^{13}C$ Analyzer (Apollo Scitech, USA). For DIC measurements, 3 mL of centrifuged media were taken and reacted within the AS-D1 analyser with 0.9 mL of a 3% H_2PO_4 and 7% NaCl solution. The absolute DIC concentration was found through quantification of the extracted CO_2 concentration as described in Deng et al. (2022). A threshold of ≤ 20 ppm pCO_2 for background synthetic air (80% N_2, 20% O_2; PanGas) was first defined. After at least 10 measurements of background air below this threshold, the stable baseline was reached and the sample is injected into the measuring chamber. As the extracted CO_2 flows into the measuring chamber, measurements of pCO_2 were taken every 3-5 seconds until all of the extracted CO_2 had passed through the measuring chamber, and the stable baseline was reached again. For the absolute DIC concentration, the integrated area of pCO_2 between the two baselines is plotted against the total DIC content. The latter is defined as the volume multiplied by the measured DIC. A Certified Reference Material, NOAA batch 186 with a known absolute DIC concentration of 2012 μM, is used for calibration. Through variation of the Certified Reference Material volume, a range of integration areas and total DIC content was obtained and internally defined. Two secondary standards with calibrated DIC concentrations were also used. Each measurement was repeated twice with the same centrifuged media in quick succession to reduce CO_2 exchange with the atmosphere, which gave an average DIC and uncertainty for each measured replicate. At least three of these replicates were taken and measured for each experiment.

For $\delta^{13}C_{DIC}$ measurements, 1 mL of centrifuged media was acidified with 150μL of 104% H_2PO_4 in a He-flushed vial. Subsequently the $\delta^{13}C_{DIC}$ was measured on a Gasbench II coupled to a Delta V Plus mass spectrometer (Thermo Fischer Scientific, USA). Two in-house $NaHCO_3$ standards dissolved in deionized water with $\delta^{13}C_{DIC}$ values of -4.66‰ and -7.94‰ were used.

The oxygen isotopic composition of the seawater ($\delta^{18}O_{sw}$) was measured on a Picarro L2130-*i* Isotope Wavelength-Scanned Cavity Ring-Down Spectrometer following Gupta et al. (2009). The water sample is first passed through a salt catchment trap, vaporized, and injected at a uniform concentration and flow rate into the Picarro spectrometer. This delivers a pulse with a constant concentration profile, during which the δ^2H and $\delta^{18}O$ are measured. Three in-house standards calibrated to three IAEA and USGS standards (SLAP2, GRESP, and VSMOW2) were run every 20 samples. Another in-house standard is run as an unknown sample. All standards fell within 1 standard deviation of their accepted value. Measurement precision was affected by the residual salt from the seawater. At least two seawater measurements were taken for each experiment. Subsequently an average $\delta^{18}O_{sw}$ and uncertainty (mean σ=0.32‰) for each condition was obtained, see Table S1. This uncertainty is used for the uncertainty of the oxygen isotope offset from seawater, $\delta^{18}O_c - \delta^{18}O_{sw}$ ($\Delta^{18}O_{c-sw}$) as reported in Table 1, and will be used in subsequent figures (mean σ=0.29‰).

pH measurements were made using a Mettler Toledo LE410 pH-probe (Mettler Toledo, Greifensee, Switzerland) and were calibrated with three NBS standards (pH=4.00, 7.01, 9.03 at 21°C), with a standard deviation of ±0.01. All pH measurements are given in the NBS scale. Seawater carbon chemistry was calculated through CO2SYS (Lewis and Wallace, 1998), with

input of measured pH and DIC, and using the K1, K2 constants of Leuker et al. (2000), KHSO$_4$ of Dickson (1990), KHF of Perez and Fraga (1987), and [B]$_I$ value of Lee et al. (2010).

255 DIC and pH measurements are compared and normalized to the initial measured values to detect potential drift and stability of the carbon chemistry of each culture. These are reported as initial DIC – measured DIC (Δ_{DIC}) and initial pH – measured pH (Δ_{pH}) in Table S1. We report the uncertainty of the fractionation between coccolith calcite and DIC ($\Delta^{13}C_{c\text{-}DIC}$) from both the standard deviation of $\delta^{13}C_c$ and the range of all measured $\delta^{13}C_{DIC}$ over the course of the sampled culture, to take into account the potential effect of DIC evolution and drift, and will be used in subsequent figures.

260 The same media was used for both batch and continuous cultures and thus the same $\delta^{13}C_{DIC}$ would be expected for both. However, through the continuous bubbling and gas-exchange in the continuous cultures, there is a potential for different $\delta^{13}C_{DIC}$ values than the batch culture setup. Indeed, there is a non-systematic enrichment of 0-1‰ for the batch culture $\delta^{13}C_{DIC}$. However, the fractionation between coccolith calcite and DIC i.e. $\Delta^{13}C_{c\text{-}DIC}$, is not affected by these differences.

An often-used index in coccolithophore geochemistry studies (McClelland et al., 2017; Phelps et al., 2021) for the relative
265 usage of carbon supply and demand is the dimensionless τ:

$$\tau = \frac{r*\rho*\mu}{3*CO_{2(aq)}*P_c} \tag{3}$$

It reflects the degree of carbon utilization by the coccolithophore as measured through growth rate (μ), defined in Eqs. 1 and 2 for batch and continuous culture setup respectively, the cell radius (r), and cellular carbon density (ρ) against the diffusive CO$_2$ supply into the cell set by (CO$_{2(aq)}$) and the permeability to CO$_2$ (P$_c$). We use a P$_c$ of 1.4 x 10^{-3} μm day^{-1} (Blanco-Ameijeiras
270 et al., 2020) and ρ of 2 x 10^{-3} μM (McClelland et al., 2017). It is assumed that there is only a diffusive supply of CO$_2$ into the cell. Our cell size measurements assume a perfect coccosphere for each counted cell, which results in a coccosphere radius that is slightly different than the cell radius. This is taken into account, together with uncertainties in μ and CO$_{2(aq)}$, into the uncertainty of the final τ value.

Pearson correlation coefficients (ρ) are used to determine whether two parameters are linearly correlated. If the ρ value is near
275 1 or -1, there is a strong correlation and one parameter has an effect on the other. Weak correlations are here defined as $\rho \leq \pm 0.40$ and significance is given by a p-value < 0.05.

3 Results

3.1 Carbon chemistry

3.1.1 DIC, pH, and CO$_{2(aq)}$

280 The stability of the carbon chemistry was monitored with at least three DIC and pH measurements for each culture. Drift from the initial conditions was less than ±20% and ±0.20 for Δ_{DIC} and Δ_{pH} respectively for 40 culture experiments (Fig. S2 and Table S1). To ensure only well-constrained culture conditions are considered, fifteen experiments with $\Delta_{DIC} \geq$20% or $\Delta_{pH} \geq$0.20 are

excluded from our main analysis in Figs. 2 through 5, but are evaluated in a subsequent comparison (see Sect. 4.3). The ranges of the well-constrained dataset ranged from 1312-5621 µM for DIC, 7.9-8.6 units for pH, and 5.6-43.8 µM for $CO_{2(aq)}$.

3.1.2 Carbon isotopes

The carbon isotope composition of the DIC ($\delta^{13}C_{DIC}$) varies between -5.10‰ and 0.80‰, with a similar large range of -5.52‰ and -0.07‰ for all species' coccolith carbon isotopes ($\delta^{13}C_c$; Table S1). This is mostly due to the large variability in $\delta^{13}C_c$ for *G. oceanica*, which can be attributed to the range of different experimental conditions. The $\delta^{13}C_c$ in *G. muellerae* varies between -4.68‰ and -3.66‰, while the $\delta^{13}C_c$ in *C. leptoporus* varies between -5.15‰ and -5.04‰.

The fractionation $\Delta^{13}C_{c-DIC}$, ranges between -1.41‰ and 1.22‰ for *G. oceanica*, -0.88‰ and 0.21‰ for *G. muellerae* and -2.86‰ and -2.22‰ for *C. leptoporus*. No significant linear correlations were identified between *Gephyrocapsa* $\Delta^{13}C_{c-DIC}$ and carbonate system parameters (DIC, pH, $CO_{2(aq)}$) or culture parameters (cell density and Δ_{DIC}) (Table S2). *Gephyrocapsa* culture data is also not significantly correlated with τ, the index of carbon demand vs supply (Fig. 2; $\rho = 0.06$, p-value = 0.74). Including *Calcidiscus* does not improve the correlation or significance with any parameter apart from Δ_{DIC}.

3.2 Oxygen isotopes

The $\delta^{18}O_{sw}$ are given in Table S1 for all cultures and vary by ~1.6‰ across with no systematic differences between batch and continuous cultures. For a given temperature, *C. leptoporus* has systematically lower $\delta^{18}O_c$ values by ~3‰ while *G. oceanica* and *G. muellerae* have similar $\delta^{18}O_c$ values at the same temperature. The interspecies variations are independent of culture setup and experimental condition.

The oxygen isotope offset from seawater, $\delta^{18}O_c - \delta^{18}O_{sw}$ ($\Delta^{18}O_{c-sw}$), varies systematically for all experimental conditions as seen in Fig. 3 and Table 1. *Calcidiscus* has a systematic offset of ~3‰ relative to *Gephyrocapsa* at the cultured growth temperatures, which agrees with previous culturing studies (Ziveri et al., 2003; Candelier et al., 2013; Stevenson et al., 2014; Hermoso et al., 2016; Katz et al., 2017). For *G. oceanica*, there is a significant negative correlation between $\Delta^{18}O_{c-sw}$ and temperature ($\rho = -0.94$, p-value <0.05), which remains when including *G. muellerae* ($\rho = -0.97$, p-value <0.05). The $\Delta^{18}O_{c-sw}$-temperature relationship is consistent between setups and experimental conditions and is not influenced by the variability in $\delta^{18}O_{sw}$ values. The available data indicate that the range of $\Delta^{18}O_{c-sw}$ is similar within the *Gephyrocapsa* genus.

3.3 Clumped isotopes

The Δ_{47} values are shown in Table 1 and Fig. 4, and range from 0.589‰ – 0.640‰ for temperatures between 12-27°C for *G. oceanica*, 0.618‰ – 0.659‰ between 6-18°C for *G. muellerae,* and 0.636‰ – 0.652‰ at 12°C for *C. leptoporus*. There is variation of ~25 ppm at given experimental conditions, in particular at 21°C and 24°C, although all datapoints fall within the long-term standard deviation of the standards used for correction of 0.020‰. There is no resolvable difference between species or genus at given temperatures; differences are within ±0.016‰ of each other.

4 Discussion

For our culture experiments, in order to evaluate whether processes promoting variable stable isotope effects would systematically affect ~~Δ_{47}~~the Δ_{47}-temperature relationship, we manipulated the media carbonate chemistry in ways that have produced variable stable isotope vital effects in coccoliths in previous cultures. We also contrasted two coccolith genera that exhibit different ranges of vital effects. Multiple physiological explanations for coccolith vital effects have been proposed (Rickaby et al., 2010; Moolna and Rickaby, 2012; Hermoso et al., 2014, 2016) and simulated previously in cellular models (Ziveri et al., 2012; Bolton and Stoll 2013; Holtz et al., 2015, 2017; McClelland et al., 2017). In our discussion, in Section 4.1 and 4.2 we briefly summarize these mechanisms, and quantify the vital effect in each experiment, so that in section 4.3 we may compare the vital effect to the Δ_{47} variations. The focus of this study is the calibration of the temperature dependence of Δ_{47} in coccolith calcite. Therefore, we will only briefly discuss the causes and mechanisms leading to isotopic disequilibrium in the cultures, focusing in particular on those that could also affect Δ_{47}.

4.1 Oxygen isotope vital effects in coccolith calcite

At a given temperature, equilibrium oxygen isotope fractionation between calcite and water is inferred to be most closely represented by natural carbonates precipitated at extremely slow rates and independent of pH (Coplen, 2007; Daëron et al., 2019). The model of Watkins et al. (2013, 2014) approximates this equilibrium, and is shown as the 'equilibrium limit' in Fig. 3. This approximation is derived from ~~their experimental setup, which is not necessarily in~~the assumed equilibrium~~, and therefore~~ of Coplen (2007), with potential small growth rate and pH effects ~~are still~~ present for carbonates not precipitated in equilibrium. Non-equilibrium fractionation effects between DIC and calcite that manifest at faster growth rates in experiments both with and without carbonic anhydrase (CA) include lower $\Delta^{18}O_{c-w}$, and a pH-dependence. This effect presumably but not necessarily occurs because calcite forms from both bicarbonate and carbonate ions in proportion to their abundance in solution. At a higher pH the proportion of calcite carbon derived from the carbonate ion increases (McConnaughey, 1989; Clark et al., 1992; Dietzel et al., 1992; Zeebe and Wolf-Gladrow, 2001; Watkins et al., 2014; Devriendt et al., 2017). Here, a pH of 8.3 at the crystallisation-site and the fastest growth rate is assumed in the model of Watkins et al. (2013, 2014) and Watkins and Devriendt (2022), with which the 'kinetic limit' is derived and illustrated in Fig. 3. This gives an approximate 2‰ offset and incorporates a large range of experimentally derived and modelled inorganic calcites precipitated in presence of CA. Additionally, numerous experiments and potentially many natural biogenic and abiogenic systems may precipitate calcite from a solution in which equilibrium between DIC and H_2O is not maintained due to a lack of CA or fast calcification rates (Devriendt et al., 2017; ~~Daëron et al. 2019).~~Guo, 2020). Rayleigh fractionation of oxygen isotopes in the internal DIC pool occurs as a result, which is transferred to the isotopic composition of the calcite and leads to lower $\Delta^{18}O_{c-w}$ values, thus exacerbating the disequilibrium fractionation potentially present between the DIC and calcite as described above.

Recent studies suggest that in certain systems such as synthetically precipitated calcite, oxygen isotope disequilibrium does not affect Δ_{47}, even for systems with intermediate oxygen isotope fractionations that fall between the kinetic and equilibrium

limits, as seen in Fig. 3 (Kelson et al., 2017; Levitt et al., 2018; Jautzy et al., 2020; Fiebig et al., 2021). Models also suggest little to no Δ_{47} disequilibrium for biogenic carbonates such as foraminifera and bivalves, as the magnitude of potential Δ_{47} disequilibrium is below the current analytical resolution for Δ_{47} measurements although this is pH and growth rate dependent (Defliese and Lohmann, 2015; Watkins and Hunt, 2015; Watkins and Devriendt, 2022). However, this does not hold for corals, brachiopods, and speleothems, where systematic $\delta^{18}O$ and Δ_{47} disequilibria are present, and should be explored further in more biogenic carbonates (Watkins and Hunt, 2015; Guo and Zhou, 2019, Guo, 2020).

Offsets from the equilibrium limit ($\Delta\Delta^{18}O_{off}$) were calculated to quantify the vital effect in oxygen isotopes. Offsets may potentially arise from pH variability, growth rate, calcification rate, or disequilibrium within the DIC-H$_2$O system. *Calcidiscus* is significantly different from equilibrium (t-test; t(4) = -58.68, p-value <0.05) and falls outside the equilibrium and kinetic limits as seen in Fig. 3. Although for *Gephyrocapsa* the mean $\Delta\Delta^{18}O_{off}$ value is around zero and there is no significant difference from the abiogenically defined equilibrium (t-test; t(72) = -0.47, p-value = 0.64), there is a range of ~1.5‰ in $\Delta\Delta^{18}O_{off}$ among different experiments. Previously published *Gephyrocapsa* data has a positive $\Delta\Delta^{18}O_{off}$ of 0-1‰ (Fig. 5; Ziveri et al., 2003; Hermoso et al., 2016).

CA has been suggested as a potential equilibration catalyst for both oxygen isotopes and Δ_{47} within the DIC-H$_2$O system in calcifying organisms. Even at an elevated pH, the equilibration time is shortened considerably for abiogenic carbonates precipitated in the presence of CA (Uchikawa and Zeebe, 2012; Kelson et al., 2017). A lack or low activity of CA can potentially cause the variable $\Delta\Delta^{18}O_{off}$ seen in our data. While the pH of the intracellular calcification site for coccoliths is not well constrained, there is experimental evidence for CA in the biomineralization pathway of *Emiliania huxleyi* (Zhang et al., 2021). Although CA has not been explicitly found in *Gephyrocapsa*, it is associated with the cytosol, chloroplast, or extracellularly in other coccolithophores (Nimer et al., 1994; Elzenga et al., 2000; Herfort et al., 2002; Rost et al., 2003). Furthermore, genes have been found associated with biomineralization and CA expression in *E. huxleyi* (Quinn et al., 2006; Soto et al., 2006; Richier et al., 2011). Models show a requirement of CA activity in the calcification pathway of coccolithophores, either in the cytosol or coccolith vesicle itself, as a purely uncatalyzed exchange would have too enriched carbon isotope values in the coccolith calcite (Holtz et al., 2015; McClelland et al., 2017). Thus, it is probable that CA is present in coccolithophores. However, the activity of CA is not well constrained so it remains uncertain whether it is sufficient to ensure full equilibration of the DIC-H$_2$O system for both oxygen isotopes and Δ_{47}.

For *Gephyrocapsa*, the 1.5‰ range in $\Delta\Delta^{18}O_{off}$ also did not correlate with pH, growth rate, DIC, CO$_{2(aq)}$, or τ (Figs. S4, S5; Table S2). The 1.5‰ range in $\Delta\Delta^{18}O_{off}$ may be explained by varying degrees of isotopic equilibration between the DIC pool and intracellular water in different experiments. Non-systematic disequilibria effects could be present for our continuous culture setup as the equilibration time for oxygen isotopic exchange between our bubbled CO$_2$ gas and the seawater media is in the order of hours (Zeebe and Wolf-Gladrow, 2001; Uchikawa and Zeebe, 2012). In support of this interpretation, there is a difference of ~0.5‰ between all continuous and batch culture $\Delta\Delta^{18}O_{off}$ (t-test; t(38) = 1.76, p-value = 0.09, Fig. 5, Table S1). Further variability in $\Delta\Delta^{18}O_{off}$ could be a result of variable intracellular pH and/or varying calcification rates as well as the presence and activity of CA. However, these physiological variations do not exhibit systematic relationships with the individual

environmental parameters such as growth rate, external pH, or carbonate system. This suggests a potential for complex co-regulation of the physiological factors and/or multiple environmental controls, which are best evaluated by cellular models and beyond the scope of this study.

4.2 Carbon isotope vital effects in coccolith calcite

In this study (Fig. 5), all continuous (and most batch) cultures for *G. oceanica* fall within the expected range of $0 \pm 1.5‰$ for $\Delta^{13}C_{c\text{-DIC}}$ as found in other studies (see Fig. S3; Rickaby et al., 2010; Moolna and Rickaby, 2012; Hermoso, 2014; Katz et al., 2017). There are no comparable culture studies for *G. muellerae*. The $\Delta^{13}C_{c\text{-DIC}}$ values fall within the range of *G. oceanica*. Both species will be combined in any inter-genera analyses for Sect. 4. *C. leptoporus* has a $\Delta^{13}C_{c\text{-DIC}}$ of $-2.0 \pm 1.0‰$ comparable to previous culturing studies (Fig. 5; Ziveri et al., 2003; Hermoso et al., 2014; Katz et al., 2017).

Models of the vital effect in coccolith carbon simulate multiple processes affecting $\Delta^{13}C_{c\text{-DIC}}$ (Bolton and Stoll, 2013; Holtz et al., 2017; McClelland et al., 2017). The carbon utilization (or demand) as a function of the supply, termed τ, is an index used to describe changes in cellular carbon uptake (relative significance of diffusive CO_2 uptake vs active HCO_3^- uptake), and depletion of the intracellular dissolved carbon pool that impact the carbon isotopic fractionation (Eq. 3, Fig. 2). The cellular calcification (particulate inorganic carbon; PIC) relative to photosynthesis (particulate organic carbon; POC) is described as the PIC:POC ratio. The PIC:POC intensity will modulate the $\Delta^{13}C_{c\text{-DIC}}$ response to τ. For moderate to heavily calcified cells with relatively high PIC:POC ratios, models simulate a decrease in $\Delta^{13}C_{c\text{-DIC}}$ with increasing τ, for example as might be triggered by decreasing concentrations of $CO_{2(aq)}$ (Eq. 3, Fig. 2). However, lightly calcified cells with PIC:POC of 0.5 exhibit a slight increase in $\Delta^{13}C_{c\text{-DIC}}$ with increasing τ, while cells with PIC:POC near 1 have $\Delta^{13}C_{c\text{-DIC}}$ nearly insensitive to τ. The *G. oceanica* in our experiments feature a range of PIC:POC ratios from 0.4 to 1.3 (Torres-Romero et al., 2024A), which likely contributes to the absence of a single clear trend between $\Delta^{13}C_{c\text{-DIC}}$ and τ. We have not determined the PIC:POC in our *Calcidiscus*, but it is generally characterized by a PIC:POC of 1.2-2.3 (Langer et al., 2006, 2012; Bolton and Stoll, 2013.). The lower $\Delta^{13}C_{c\text{-DIC}}$ of *Calcidiscus* correlate with lower $\Delta\Delta^{18}O_{off}$ (Figure 5), as observed in size fractions from sediments (e.g. Bolton and Stoll, 2013), but the physiological mechanism of this correlation has not yet been quantitatively explored in a coupled model of carbon and oxygen isotope fractionation in coccoliths.

4.3 Calibration of coccolith clumped isotopes and temperature

Despite the significant vital effects in carbon and oxygen isotopes, our coccolith Δ_{47} values show a consistent relationship with temperature (Fig. 6), which is similar to previous calibration studies (see Sect. 4.4, 4.5). In order to calculate a reliable coccolith Δ_{47}-temperature regression, we used a simple least-squares fitting following Williamson (1968) and York et al. (2004), using the Excel spreadsheet by Cantrell (2008). This methodology considers the uncertainties from both the Δ_{47} and temperature measurements. While the omni-variant generalised least squares regression would be better suited, as this incorporates the full error covariance (Daëron and Vermeesch, 2024), our data is standardised through reference materials in a moving time window and thus cannot be analysed through this method. As pointed out in a number of studies (Bonifacie et al., 2017; Fernandez et

al., 2017; Katz et al., 2017; Kelson et al., 2017; de Winter et al., 2022), the bias from a low number of analytical replicates and the small temperature range can lead to significant differences in calibration slope and intercepts. In order to determine potential species- or genus-dependent effects, an unorthodox approach was initially tested. *G. oceanica* contains the most diverse and largest range of temperature datapoints, while *C. leptoporus* only contains one temperature point and three Δ_{47}

415   data points. Thus, the other two species' datasets will be successively included and evaluated for significance relative to the *G. oceanica* dataset. Further, each biological and technical Δ_{47} sample and uncertainty are taken individually as to have an equal contribution of each datapoint to the final calibration. The initial uncertainty of 0.1°C for temperature is 0.018 K^{-2} after conversion to 1/T^2. The resulting slopes and intercepts of the Δ_{47}-temperature regressions are seen in Table 2~~.~~, with corresponding errors. With the successive inclusion of the two other species, there is no significant change or offset in slope

420   or intercept relative to the initial *G. oceanica* regression. All regression lines fall within 0.0012‰ error of each other, which shows that with the available data and at the current analytical precision there is no discernible species- or genus-specific vital effect ~~on~~that affects the Δ_{47}-temperature relationship.

Secondly, we tested the potential influence of variable carbonate chemistry and the carbon and oxygen "vital effects" on the Δ_{47}-temperature relationship. To this end, we normalized our Δ_{47} data against the Meinicke et al. (2020) Δ_{47}-temperature

425   calibration at each temperature to generate residual values ($\Delta\Delta_{47,off}$). Pearson correlation tests were then performed for the normalized $\Delta\Delta_{47,off}$ residual values against the different carbonate chemistry parameters. The resulting Pearson correlation coefficients are shown in Table 3. Apart from a weak non-significant, positive and negative correlation for the batch and continuous culture setup $\Delta\Delta_{47,off}$ and pH respectively and a moderate but significant positive correlation between the continuous culture setup $\Delta\Delta_{47,off}$ and $\Delta\Delta^{18}O_{off}$, there are no conclusive or significant correlations for all measurements and

430   experimental setups. There is no significant difference in the normalized $\Delta\Delta_{47,off}$ values between batch and continuous culture setups (t-test; t(38) = 0.35, p-value = 0.73), further indicating that carbonate chemistry does not have an effect on the measured Δ_{47} value. The non-significant correlation in $\Delta^{13}C_{c\text{-}DIC}$ and $\Delta\Delta_{47,off}$ for all setups~~,~~ shows that ~~there is no~~the processes responsible for the carbon isotope vital effect ~~affecting~~do not significantly influence the coccolith Δ_{47}-~~values~~temperature relationship (Fig. S6). While there is a moderate, significant positive correlation between $\Delta\Delta^{18}O_{off}$-$\Delta\Delta_{47,off}$, it is only present for the continuous

435   culture setup and has an r^2 of 0.20. Thus, there is no evidence of an important impact of the oxygen isotope vital effect on coccolith Δ_{47}-values.

Thirdly, average Δ_{47} values were calculated for each species at every growth temperature. These temperature-weighted averages can highlight bias from a low number of measurement replicates at certain growth temperatures, such as at 6°C and 27°C. The resulting Δ_{47}-temperature regression is indistinguishable from regressions using individual Δ_{47} sample datapoints

440   (±6.1 ppm; Table 2).

Lastly, if there are no species-specific nor carbonate chemistry related vital effects in the Δ_{47}-temperature relationship, the data that were initially excluded due to the poorly characterized carbonate system (see Sect. 3.1.1) and poor constraining of the stable carbon and oxygen isotope fractionations (i.e. datapoints with $\Delta_{DIC} \geq 20\%$ or $\Delta_{pH} \geq 0.20$) can also be included. If the Δ_{47}-temperature relationship in coccoliths is purely related to temperature, this will not interfere with the resulting calibration.

445 Indeed, the slope and intercept fall within error of the other regressions, albeit with a slightly higher slope and lower intercept, seen in Table 2 and Fig. 6.

Based on the above analysis we conclude that all 55 datapoints can be considered for a coccolith Δ_{47}-temperature calibration (T in K, $\pm 1\sigma$):

$$\Delta_{47}(I - CDES) = 0.0375 \pm 0.004 * \frac{10^6}{T^2} + 0.181 \pm 0.048 \tag{4}$$

450 **4.4 A unified coccolith Δ_{47}-temperature calibration?**

The similar culturing study of three coccolithophore species by Katz et al. (2017) also found ~~no~~that species-specific vital effects ~~affecting~~do not correlate with variations in the Δ_{47} ~~values~~ temperature relationship and also found a consistent Δ_{47}-temperature correlation. However, the study was conducted before the introduction of the I-CDES standardisation methodology using carbonates and used gas-based standardization, consequently the data could have a systematic difference that cannot be resolved with certainty. Thus, when comparing to other calibration studies we will not include Katz et al. (2017)

455 in the dataset and use Eq. 4 as a coccolith Δ_{47}-temperature calibration, which is only based on our culture data in the I-CDES frame.

4.5 A coccolith or biogenic specific calibration?

In Fig. 7 and 8 we compare our data with previous biogenic and inorganic carbonate Δ_{47}-temperature studies, with the method

460 of temperature measurement or estimations in Table 4. The slopes and the intercepts of the equations with a limited number of replicates and a limited range of temperatures have larger uncertainties (Bonifacie et al., 2017; Fernandez et al., 2017; Kelson et al., 2017) and all datasets have a significant scatter due to their small variability. ~~We focus on five biogenic (Peral et al., 2018; Meinicke et al., 2020; Caldarescu et al., 2021; de Winter et al., 2022; Huyghe et al., 2022) and one inorganic ("MIT calibration"; Anderson et al., 2021; Daëron and Gray, 2023) carbonate studies. All datasets are converted to I-CDES~~

465 ~~using the methodology described in Bernasconi et al. (2021). The biogenic data sets are combined into a general 'biogenic' calibration, excluding this study. The dataset of Caldarescu et al. (2021) is included in the de Winter et al. (2022) calibration, using their equation 3. As suggested by Huyghe et al. (2022), the juvenile specimen that shows Δ_{47} disequilibrium effects related to growth rate is not included. The planktic foraminifera data recalculated to I-CDES of Meinicke et al. (2020) and Peral et al. (2018) are combined. Both the original studies' and recalculated calcification temperatures by Daëron and Gray~~

470 ~~(2023) are used, and named 'Daëron & Gray 2023 orig' and 'Daëron & Gray 2023 recal' respectively.~~If the data is not in I-CDES already, the datasets are converted to I-CDES using the methodology described in Bernasconi et al. (2021).

While overall the individual Δ_{47} values for coccolith calcite fall within the scatter of the previous calibrations, our coccolith Δ_{47}-temperature regression plots systematically above. To identify and evaluate how this would impact temperature reconstructions, a similar exercise to Sect. 4.3 was performed. At all growth temperatures, a Δ_{47} value was calculated from

475 each calibration. $\Delta\Delta_{47,off}$ residuals were then generated through comparison with our study's calibration at each temperature.

All non-coccolith calibrations yield negative residuals ($\Delta\Delta_{47,off}$) relative to our coccolith Δ_{47}-temperature calibration. This results in lower calculated Δ_{47} temperatures compared to our calibration (Fig. 8). Positive offsets were found for aragonite (de Winter et al., 2022) and brachiopods (Bajnai et al., 2018; Davies et al., 2023; Letulle et al. 2023), when compared to the Anderson et al. (2021) inorganic carbonate calibration. However, brachiopods show a complex system of kinetic disequilibrium effects in both Δ_{47} and Δ_{48} associated with early-stage CO_2 absorption in the DIC, and do not have the CA enzyme. de Winter et al. (2022), in addition, argued that the Δ_{47}-temperature relationship is non-linear at temperatures >100°C and calibrations are substantially biased by data with a large temperature range such as Anderson et al. (2021) when used at temperatures <30°C. The 'MIT' calibration uses only the inorganic carbonates from the Anderson et al. (2021) dataset and indeed yields lower and non-overlapping $\Delta\Delta_{47,off}$ residuals relative to our calibration (Fig. 8). Using only the data <30°C from Anderson et al. (2021) to calculate a temperature regression does yield overlapping $\Delta\Delta_{47,off}$ residuals relative to our calibration, however due to the steeper slope of the calibration, the $\Delta\Delta_{47,off}$ residuals are strongly temperature dependent. The non-linearity of the Δ_{47}-temperature relationship is thus most likely not a major cause for the consistent offset of our coccolith calibration (see Table S3).

Both the variability and absolute $\Delta\Delta_{47,off}$ residuals differ for all compared calibrations. The Daëron and Gray (2023) and MIT calibrations yield $\Delta\Delta_{47,off}$ residuals that do not overlap with our dataset between 2-28°C. The original Peral et al. (2018; 2022), Meinicke et al. (2020; 2021), de Winter et al. (2022), and Huyghe et al. (2022) calibrations do yield $\Delta\Delta_{47,off}$ residuals within the uncertainty of our dataset. Temperature offsets at the average growth temperature of our dataset, 18.7°C, are between 0°C and 4°C for the different calibrations, but vary in magnitude at different temperatures, see Table 4.

The high variability of the temperature offsets over the given temperature range for certain biogenic carbonate studies such as de Winter et al. (2022), suggest non-uniform disequilibrium effects are present. As such, two conclusions can be derived and discussed; there is a coccolith specific-calibration or the calcification temperatures for previous studies are underestimated. Our well-constrained coccolith cultures allow for the exclusion of effects from environmental variabilities, such as $CO_{2(aq)}$ (here between 5.6 and 43.8 μM), pH (here between 7.9 and 8.6 units), coccolithophore growth rate, and vital effects on Δ_{47} values as discussed in Sect. 4.3. The processes responsible for vital effects observed in the coccolith carbon and oxygen isotopes do not lead to corresponding variations in the Δ_{47}-temperature relationship, where $\Delta\Delta_{47,off}$ are within 0.0012‰ despite up to ~3‰ variability for carbon and oxygen isotopes for our experimental conditions. This is below our analytical uncertainty for Δ_{47}, thus while we can't fully rule out that vital effects do not affect coccolith $\Delta\Delta_{47,off}$ residuals, the offset from the inorganic equilibrium calibration must be similar at all temperatures, systematic, and unrelated to vital effects. Indeed, for the available dataset and range in carbonate chemistry no species- or genus-related effects are present, although this must be further examined in future studies with in situ temperatures such as sediment traps or cultures with a wider range in seawater chemistry. To a certain degree, ~~offsets are~~another potential cause for offset of our coccolith to previous biogenic carbonate calibrations is also likely due to the uncertainty related to the determination of calcification temperatures in previous calibrations based on foraminifera collected from core tops. Often indirectly inferred or estimated from other proxies, these uncertainties in the calcification temperatures can result in large variabilities, obscure potential effects related to temperature, and can result in

510 differences between calibrations. In particular, there is no directly measured constraint on the calcification temperatures, only inference and empirical relationships from other proxies. Meinicke et al. (2020) compared and discussed three different methods of determining the calcification temperature of the foraminifera used in their study, and concluded that using their oxygen isotope composition and the temperature calibration of Shackleton et al. (1974) provides the most robust estimate of the true calcification temperatures. In an extensive study, Daëron and Gray (2023) re-determined the oxygen isotope

515 fractionation in the foraminifera species that were used by Meinicke et al. (2020; 2021) and Peral et al. (2018; 2022) for their clumped isotope calibrations using ~~samples~~data from foraminifera from laboratory cultures and plankton tows. They concluded that foraminifera calcification temperatures are best approximated by using the Kim and O'Neil (1997) calibration with species-specific offsets. They tested this concept by comparing the calcification temperatures determined for the Meinicke et al. (2020; 2021) and Peral et al. (2018; 2022) datasets, with reconstructed water column temperatures at the sites of the core

520 tops (Fig. 7 in Da~~e~~ëron and Gray, 2023), and concluded that this is a better estimate of calcification temperatures than previously published. The applications of these revised species-specific oxygen isotope fractionation curves result in a non-systematic 1-2°C offset to colder temperatures from the original studies of Peral et al. (2018; 2022) and Meinicke et al. (2020; 2021 ; Fig. 8), especially at temperatures below 15°C and leads to a ~~match~~coincidence between these two foraminifera-based calibrations and the inorganic calibration of Anderson et al. (2021). A close examination of Fig 7 in Da~~e~~ëron and Grey (2023)

525 however, shows that the majority of their discordant samples (i.e. those that record temperatures outside the measured water column temperatures at the living depth of the specific species) are on the cold part of the calibration, 12 are below 13°C. Moreover, at least 7 of the ones that are considered concordant as the error bars overlap with the measured temperatures, have an average that is 1-2°C below the lowest measured temperature. About 27 of the 37 datapoints below 15 °C are either colder than the lowest temperature or only overlap with the coldest temperatures of the observed water column temperature range.

530 We suggest that this would impart a cold bias on those samples. Further, the proposed extension of the calcification depths to 500 m would also give a cold bias and is not supported by foraminifera living depths (Schiebel and Hembleben, 2017). Based on these considerations, we suggest that the use of calcification temperatures from oxygen isotopes need further testing, ideally on laboratory cultured specimens and warrants caution and consideration.

~~Both the variability and absolute ΔΔ$_{47,off}$ residuals differ for all compared calibrations. The Daëron and Gray (2023) and MIT~~
535 ~~calibrations yield ΔΔ$_{47,off}$ residuals that do not overlap with our dataset between 2-28°C. The original Peral et al. (2018),~~
~~Meinicke et al. (2020), de Winter et al. (2022), and Huyghe et al. (2022) calibrations do yield ΔΔ$_{47,off}$ residuals within the~~
~~uncertainty of our dataset. Temperature offsets at the average growth temperature of our dataset, 18.7°C, are between 0°C and~~
~~4°C for the different calibrations, but vary in magnitude at different temperatures, see Table 4.~~

~~The high variability of the temperature offsets over the given temperature range for certain biogenic carbonate studies such as~~
540 ~~de Winter et al. (2022), suggest non-uniform disequilibrium effects are present. Thus, a pooled calibration including all~~
~~biogenic studies mentioned, except this study, and using either the original and recalculated calcification temperatures were~~
~~performed to identify whether there is potential for a general biogenic specific calibration (Fig. 8). Our dataset still has a~~
~~positive ΔΔ$_{47,off}$ relative to the biogenic calibrations, for the original calcification temperatures from 2°C to 1.5°C for 27°C to~~

The tightly-controlled growth temperatures of our coccolithophore cultures eliminate the problem of uncertain calcification temperatures as in the case of foraminifera calibrations (Meinicke et al., 2020; Daëron and Gray, 2023). Indeed, the offsets of our coccolith calibration relative to the inorganic MIT calibration are consistent, with little variability, and suggest a uniform disequilibrium mechanism ($\Delta\Delta_{47,off}$ = -0.0079±0.0005‰). The purely foraminifera-based calibrations, using both the original and recalculated calcification temperatures of Peral et al. (2018; 2022) and Meinicke et al. (2020; 2021), show more variability relative to the inorganic MIT calibration ($\Delta\Delta_{47,off}$ = 0.0023±0.0012‰ and $\Delta\Delta_{47,off}$ = -0.0013±0.0015‰ respectively), and suggests variable disequilibrium effects. However, at this stage it is difficult to state whether this is due to general foraminifera, species-specific disequilibria, or due to uncertainties related to the calcification temperature. This highlights the importance and uncertainties related to the calcification temperature and their implications.

Modelling studies for inorganic calcite, grown in the presence of CA and at growth rates and pH ranges relevant for coccolithophores, show offsets for carbon and oxygen and find kinetic disequilibrium effects that are pH and crystal-growth rate dependent (Hill et al., 2014; Watkins and Hunt, 2015; Uchikawa et al., 2021; Watkins and Devriendt, 2022). Between our cultured temperatures of 6-27°C and in saline conditions, a shift from pH 8 to 8.5 can give an offset of ~3‰ for $\delta^{18}O$ and ~90 ppm for Δ_{47} at very fast crystal growth rates (10^{-5} mol m^{-2}s^{-1}) and offsets of ~1‰ for $\delta^{18}O$ and ~1 ppm for Δ_{47} for 1000x slower crystal growth rates (10^{-7} mol m^{-2}s^{-1}; Fig. 6 in Watkins and Devriendt, 2022). The latter is comparable to estimated coccolith calcification rates of 10^{-7}-10^{-8} mol m^{-2}s^{-1} (Langer et al., 2006, 2012; Sett et al., 2014). Also, the modelled difference of Δ_{47} between HCO_3^- relative to CO_3^{2-} at 25°C, with a difference of ~5 pH units, and saline conditions is ~0.034‰, and ~7‰ for $\delta^{18}O$ (Hill et al., 2014; Watkins and Devriendt, 2022). Thus, the difference due to calcification mechanisms by regulating internal pH and thus the HCO_3^-/CO_3^{2-} ratio that has been postulated to drive the carbon and oxygen vital effect differences between different coccolithophore and foraminifera species cannot be applied on its own to explain the Δ_{47} offset from equilibrium (Spero et al., 1997; Rickaby et al., 2010; Ziveri et al., 2012; Devriendt et al., 2017; Holtz et al., 2017). Rather, a crystal growth rate variability between species is likely the cause of the 3‰ offset in $\Delta\Delta^{18}O_{off}$ between *C. leptoporus* and *G. oceanica* and only ±1.2 ppm difference in Δ_{47}. Perhaps, a difference due to species-specific coccolith-associated-proteins and

CAPs that can influence different calcite saturation states within the coccolith vesicle and lead to more crystal-growth rate variability, can also have an effect (Lee et al., 2016). However, asGal et al., 2016; Lee et al., 2016; Walker et al., 2019). Other

580 effects may also be at play, such as species-specific metabolic pathways unique to coccolithophores, diffusion of cations or DIC species into the coccolith vesicle, surface speciation, or crystal surface interactions with cations from solution (Hermoso, 2014; Sand et al., 2014; Gal et al., 2017; Taylor et al., 2017). However, while the offset from the equilibrium inorganic calcite is systematic across the three coccolithophore species cultured here, no definitive cause of this observed offset can be definitively determined in this study, and there is more work needed to identify the disequilibrium processes for other

585 coccolithophore species as well as for foraminifera.. Future studies with constrained and in situ temperature measurements such as in sediment traps (Clark et al., 2024) or cultures are recommended to disentangle and validate our findings of this biogeniccoccolith clumped isotope disequilibrium.

5 Conclusions

In this study we cultured three species of coccolithophores (*Gephyrocapsa oceanica*, *G. muellerae*, and *Calcidiscus*

590 *leptoporus*) in continuous and batch culture setups for temperatures between 6 and 27°C and $CO_{2(aq)}$ between 5 and 45 μM. Vital effects in carbon and oxygen isotopes in coccoliths were observed and their magnitude is consistent with previous culturing studies. We show that for our well-constrained continuous culture setup there are no systematic external environmental influences from pH, DIC, or $CO_{2(aq)}$ on the carbon and oxygen isotopic values for both *G. oceanica* and *G. muellerae*. Both species precipitate coccolith calcite close to isotopic equilibrium with the water ($\Delta^{13}C_{c\text{-}DIC} = \pm1.5‰$; $\Delta\Delta^{18}O_{off}$

595 $= \pm1‰$). *C. leptoporus* shows pronounced vital effects in both carbon and oxygen isotopes, although no clear physiological conclusions can be drawn on the source of these vital effects. A calcification model would aid in describing the sources of the vital effects.

We establish a coccolith-specific Δ_{47}-temperature calibration and observe a consistent offset from previous inorganic calibrations ($\Delta\Delta_{47,off} = -0.0079\pm0.0005‰$), which suggests disequilibrium effects in coccolith Δ_{47} for all three coccolithophore

600 species. There are however, no effects on the calibration that are due to differences in environmental parameters or species. Our coccolith Δ_{47} data is largely consistent with a previous coccolith culture study (Katz et al., 2017), and indicates that coccolithophores precipitate coccolith calcite in clumped isotope disequilibrium with their environment. Our well constrained coccolith Δ_{47}-temperature calibration (Eq. 4)4), with well-constrained temperatures, also shows offsets from previous biogenic carbonate calibration studies, dependent on the choice of calcification temperature. The discrepancies derived from the

605 differences in calcification temperature render it difficult to conclusively state whether a general biogenic calibration should be used.. Thus, we suggest the use of our well constrainedcoccolith Δ_{47}-temperature calibration to reconstruct temperatures from well screened/preserved coccolith calcite, regardless of species.

Author contributions.

AJC: cell culture, analyses, and writing, ITR: cell culture and analyses, MJ: analyses, SMB: supervision, analyses, funding acquisition, and writing, HMS: supervision, funding acquisition, and writing.

Competing interests

The authors declare that they have no conflict of interest.

Acknowledgements

The authors thank Anne-Greet Bittermann of ScopeM for their support and assistance in this work. This work was supported by ETH core funding (ETH-02 21-1) and SNF grant (no. 200021_182070). We would like to thank two anonymous reviewers for their constructive comments.

References

Anderson, N., Kelson, J., Kele, S., Daëron, M., Bonifacie, M., Horita, J., Mackey, T., John, C., Kluge, T., Petschnig, P., Jost, A., Huntington, K., Bernasconi, S., Bergmann, K.: A Unified Clumped Isotope Thermometer Calibration (0.5–1,100°C) Using Carbonate-Based Standardization, Geophys Res Lett, 48(7), 10.1029/2020GL092069, 2021.

Bach, L., MacKinder, L., Schulz, K., Wheeler, G., Schroeder, D., Brownlee, C., and Riebesell, U.: Dissecting the impact of CO_2 and pH on the mechanisms of photosynthesis and calcification in the coccolithophore Emiliania huxleyi, New Phytol, 199(1), 121-134, 10.1111/nph.12225, 2013.

Bajnai, D., Fiebig, J., Tomašových, A., Milner Garcia, S., Rollion-Bard, C., Raddatz, J., Löffler, N., Primo-Ramos, C., Brand, U.: Assessing kinetic fractionation in brachiopod calcite using clumped isotopes, Scientific Reports, 8(533), 10.1038/s41598-017-17353-7, 2018.

Barry, J., Hall-Spencer, J., and Tyrrell, T.: In situ perturbation experiments: natural venting sites, spatial/temporal gradients in ocean pH, manipulative in situ pCO2 perturbations, in: Guide to best practices for ocean acidification research and data reporting, edited by: U. Riebesell, V. Fabry, L. Hansson, and Gattuso J.-P., Office for Official Publications of the European Communities, Luxembourg, 123-136, 10.2777/66906, 2012.

Berger, W.: Deep-sea carbonates: evidence for a coccolith lysocline, Deep-Sea Res, 20, 917-921, 1973.

Berman, A., Hanson, J., Leiserowitz, L., Koetzle, T., Weiner, S., and Addadi, B.: Biological Control of Crystal Texture: A Widespread Strategy for Adapting Crysta Properties to Function, Science, 259, 776-779, 10.1126/science.259.5096.776, 1993.

Bernasconi, S., Hu, B., Wacker, U., Fiebig, J., Breitenbach, S., and Rutz, T.: Background effects on Faraday collectors in gas-source mass spectrometry and implications for clumped isotope measurements. Rapid Commun Mass Sp, 27(5), 603-612, 10.1002/rcm.6490, 2013.

Bernasconi, S., Müller, I., Bergmann, K., Breitenbach, S., Fernandez, A., Hodell, D., Jaggi, M., Meckler, A., Millan, I., and Ziegler, M.: Reducing Uncertainties in Carbonate Clumped Isotope Analysis Through Consistent Carbonate-Based Standardization, Geochem Geophy Geosy, 19(9), 2895-2914, 10.1029/2017GC007385, 2018.

Bernasconi, S., Daëron, M., Bergmann, K., Bonifacie, M., Meckler, A., Affek, H., Anderson, N, Bajnai, D., Barkan, E., Beverly, E., Blamart, D., Burgener, L., Calmels, D., Chaduteau, C., Clog, M., Davidheiser-Kroll, B., Davies, A., Dux, F., Eiler, J., Elliott, B., Fetrow, A., Fiebig, J., Goldberg, S., Hermoso, M., Huntington, K., Hyland, E., Ingalls, M., Jaggi, M., John, C., Jost, A., Katz, S., Kelson, J., Kluge, T., Kocken, I., Laskar, A., Leutert, T., Liang, D., Lucarelli, J., Mackey, T., Mangenot, X., Meinicke, N., Modestou, S., Muller, I., Murray, S., Neary, A., Packard, N., Passey, B., Pelletier, E., Petersen, S., Piasecki, A., Schauer, A., Snell, K.E., Swart, P., Tripati, A., Upadhyay, D., Vennemann, T., Winkelstern, I., Yarian, D., Yoshida, N., Zhang, N., and Ziegler, M.: InterCarb: A Community Effort to Improve Interlaboratory Standardization of the Carbonate Clumped Isotope Thermometer Using Carbonate Standards, Geochem, Geophy, Geosy, 22(5), 10.1029/2020GC009588, 2021.

Blanco-Ameijeiras, S., Stoll, H., Zhang, H., and Hopkinson, B.: Influence of temperature and CO2 on plasma-membrane permeability to CO2 and HCO3- in the marine haptophytes Emiliania huxleyi and Calcidiscus leptoporus (Prymnesiophyceaea), J Phycol, 56, 1283-1294, doi/10.1111/jpy.13017, 2020.

Bolton, C., and Stoll, H.: Late Miocene threshold response of marine algae to carbon dioxide limitation, Nature, 500(7464), 558-562, 10.1038/nature12448, 2013.

Bonifacie, M., Calmels, D., Eiler, J., Horita, J., Chaduteau, C., Vasconcelos, C., Agrinier, P., Katz, A., Passey, B., Ferry, J., and Bourrand, J.: Calibration of the dolomite clumped isotope thermometer from 25 to 350 °C, and implications for a universal calibration for all (Ca, Mg, Fe)CO3 carbonates, Geochim Cosmochim Ac, 200, 255-279, 10.1016/j.gca.2016.11.028, 2017.

Brownlee, C., Wheeler, G., Taylor, A. Coccolithophore biomineralization: New questions, new answers, Semin Cell Dev Biol, 46, 11-16, 10.1016/j.semcdb.2015.10.027, 2015.

Caldarescu, D., Sadatzki, H., Andersson, C., Schafer, P., Fortunato, H., Meckler, A.: Clumped isotope thermometry in bivalve shells: A tool for reconstructing seasonal upwelling, Geochim Cosmochim Ac, 294, 174-191, 10.1016/j.gca.2020.11.019, 2021.

Candelier, Y., Minoletti, F., Probert, I., and Hermoso, M.: Temperature dependence of oxygen isotope fractionation in coccolith calcite: A culture and core top calibration of the genus Calcidiscus, Geochim Cosmochim Ac, 100, 264-281, 2013.

Cantrell, C.: Technical Note: Review of methods for linear least-squares fitting of data and application to atmospheric chemistry problems, Atmos Chem Phys, 8(17), 5477-5487, 10.5194/acp-8-5477-2008, 2008.

Clark, A., Jaggi, M., Bernasconi, S., and Stoll, H.: Do coccolith clumped isotopes record sea surface temperatures? A sediment trap perspective, EGU General Assembly 2024, Vienna, Austria, 14–19 Apr 2024, EGU24-15587, 10.5194/egusphere-egu24-15587, 2024.

Clark, I., Fontes, J., and Fritz, P.: Stable isotope disequilibria in travertine from high pH waters: Laboratory investigations and field observations from Oman, Geochim Cosmochim Ac, 56, 2041-2050, https://doi.org/10.1016/0016-7037(92)90328-G, 1992.

Coplen, T.: Calibration of the calcite-water oxygen-isotope geothermometer at Devils Hole, Nevada, a natural laboratory, Geochim Cosmochim Ac, 71(16), 3948-3957, 10.1016/j.gca.2007.05.028, 2007.

Daëron, M.: Full Propagation of Analytical Uncertainties in $\Delta 47$ Measurements, Geochem Geophy Geosy, 22(5), 10.1029/2020GC009592, 2021.

Daëron, M., and Gray, W.: Revisiting oxygen-18 and clumped isotopes in planktic and benthic foraminifera, Paleoceanography and Paleoclimatology, 38(10), 2023-2032, 10.1029/2023PA004660, 2023.

Daëron, M., and Vermeesch, P.: Omnivariant Generalized Least Squares regression: Theory, geochronological applications, and making the case for reconciled $\Delta 47$ calibrations, Chem Geol, 647, 10.1016/j.chemgeo.2023.121881, 2024.

Daëron, M., Blamart, D., Peral, M., and Affek, H.: Absolute isotopic abundance ratios and the accuracy of $\Delta 47$ measurements, Chem Geol, 442, 83-96, 10.1016/j.chemgeo.2016.08.014, 2016.

Daëron, M., Drysdale, R., Peral, M., Huyghe, D., Blamart, D., Coplen, T., Lartaud, F., and Zanchetta, G.: Most Earth-surface calcites precipitate out of isotopic equilibrium, Nature Commun, 10(1), 10.1038/s41467-019-08336-5, 2019.

Davies, A., Guo, W., Bernecker, M., Tagliavento, M., Raddatz, J., Gischler, E., Flögel, S., Fiebig, J.: Dual clumped isotope thermometry of coral carbonate, Geochim Cosmochim Ac, 338, 66–78. 10.1016/j.gca.2022.10.015, 2022.

Davies, A., Brand, U., Tagliavento, M., Bitner, M., Bajnai, D., Staudigel, P., Bernecker, M., Fiebig, J.: Isotopic disequilibrium in brachiopods disentangled with dual clumped isotope thermometry, Geochim Cosmochim Ac, 359, 135–147. 10.1016/j.gca.2023.08.005, 2023.

de Winter, N., Witbaard, R., Kocken, I., Müller, I., Guo, J., Goudsmit, B., and Ziegler, M.: Temperature Dependence of Clumped Isotopes ($\Delta 47$) in Aragonite, Geophys Res Lett, 49(20), 10.1029/2022GL099479, 2022.

Defliese, W., and Lohmann, K.: Non-linear mixing effects on mass-47 CO_2 clumped isotope thermometry: Patterns and implications, Rapid Commun Mass Sp, 29(9), 901-909, 10.1002/rcm.7175, 2015.

Deng, X., Li, Q., Su, J., Liu, C., Atekwana, E., and Cai, W.: Performance evaluations and applications of a $\delta 13C$-DIC analyzer in seawater and estuarine waters, Sci Total Environ, 833, 10.1016/j.scitotenv.2022.155013, 2022.

Dennis, K., and Schrag, D.: Clumped isotope thermometry of carbonatites as an indicator of diagenetic alteration, Geochim Cosmochim Ac, 74(14), 4110-4122, 10.1016/j.gca.2010.04.005, 2010.

Devriendt, L., Watkins, J., and McGregor, H.: Oxygen isotope fractionation in the $CaCO_3$-DIC-H_2O system, Geochim Cosmochim Ac, 214, 115-142, 10.1016/j.gca.2017.06.022, 2017.

Dickson, A.: Standard potential of the reaction: $AgCl(s) + 1/2H_2(g) = Ag(s) + HCl(aq)$, and the standard acidity constant of the ion HSO_4^- in synthetic sea water from 273.15 to 318.15 K. J Chem Thermodyn, 22, 113-127, 10.1016/0021-9614(90)90074-Z, 1990.

Dietzel, M., Usdowski, E., and Hoefst, J.: Chemical and 13C/12C- and 18O/16O-isotope evolution of alkaline drainage waters and the precipitation of calcite, Appl Geochem, 7, 177-184, 10.1016/0883-2927(92)90035-2, 1992.

Drury, A., and John, C.: Exploring the potential of clumped isotope thermometry on coccolith-rich sediments as a sea surface temperature proxy, Geochem Geophy Geosy, 17(10), 4092-4104, 10.1002/2016GC006459, 2016.

Eiler, J.: "Clumped-isotope" geochemistry-The study of naturally-occurring, multiply-substituted isotopologues, Earth Planet Sc Lett, 262(3-4), 309-327, 10.1016/j.epsl.2007.08.020, 2007.

Eiler, J., and Schauble, E.: 18O13C16O in Earth's atmosphere, Geochim Cosmochim Ac, 68(23), 4767-4777, 10.1016/j.gca.2004.05.035, 2004.

Elzenga, J., Prins, H., and Stefels, J.: The role of extracellular carbonic anhydrase activity in inorganic carbon utilization of Phaeocystis globosa (Prymnesiophyceae): A comparison with other marine algae using the isotopic disequilibrium technique, Limnol Oceanogr, 45(2), 372-380, 10.4319/lo.2000.45.2.0372, 2000.

Falster, G., Delean, S., and Tyler, J.: Hydrogen Peroxide Treatment of Natural Lake Sediment Prior to Carbon and Oxygen Stable Isotope Analysis of Calcium Carbonate, Geochem Geophy Geosy, 19(9), 3583-3595, 10.1029/2018GC007575, 2018.

Fernandez, A., Müller, I., Rodríguez-Sanz, L., van Dijk, J., Looser, N., and Bernasconi, S.: A Reassessment of the Precision of Carbonate Clumped Isotope Measurements: Implications for Calibrations and Paleoclimate Reconstructions, Geochem Geophy Geosy, 18(12), 4375-4386, 10.1002/2017GC007106, 2017.

Fiebig, J., Daëron, M., Bernecker, M., Guo, W., Schneider, G., Boch, R., Bernasconi, S., Jautzy. J., Dietzel, M.: Calibration of the dual clumped isotope thermometer for carbonates, Geochim Cosmochim Ac, 312, 235-256, 10.1016/j.gca.2021.07.012, 2021.

Frølich, S., Sørensen, H., Hakim, S., Marin, F., Stipp, S., and Birkedal, H.: Smaller calcite lattice deformation caused by occluded organic material in coccoliths than in mollusk shell, Cryst Growth Des, 15(6), 2761-2767, 10.1021/acs.cgd.5b00118, 2015.

Gal, A., Wirth, R., Kopka, J., Fratzl, P., Faivre, D., Scheffel, A. Macromolecular recognition directs calcium ions to coccolith mineralization sites, Science, 353(6299), 590-593, 10.1126/science.aaf7889, 2016.

Gal, A., Sviben, S., Wirth, R., Schreiber, A., Lasalle-Kaiser, B., Faivre, D., Scheffel, A. Trace-Element Incorporation into Intracellular Pools Uncovers Calcium-Pathways in a Coccolithophore, Adv Sci, 4(10), 1700088, 10.1002/advs.201700088, 2017.

Ghosh, P., Adkins, J., Affek, H., Balta, B., Guo, W., Schauble, E., Schrag, D., Eiler, J.: 13C-18O bonds in carbonate minerals: A new kind of paleothermometer, Geochim Cosmochim Ac, 70(6), 1439-1456, 10.1016/j.gca.2005.11.014, 2006.

Guo, W.: Kinetic clumped isotope fractionation in the DIC-H2O-CO2 system: Patterns, controls, and implications, Geochim Cosmochim Ac, 268, 230-257, 10.1016/j.gca.2019.07.055, 2020.

Guo, W., and Zhou, C.: Patterns and controls of disequilibrium isotope effects in speleothems: Insights from an isotope-enabled diffusion-reaction model and implications for quantitative thermometry, Geochim Cosmochim Ac, 267, 196-226, 10.1016/j.gca.2019.07.028, 2019.

735 Gupta, P., Noone, D., Galewsky, J., Sweeney, C., and Vaughn, B.: Demonstration of high-precision continuous measurements of water vapor isotopologues in laboratory and remote field deployments using wavelength-scanned cavity ring-down spectroscopy (WS-CRDS) technology, Rapid Commun Mass Sp, 23(16), 2534-2542, 10.1002/rcm.4100, 2009.

Henriksen, K., Young, J., Brown, P., & Stipp, S.: Coccolith biomineralisation studied with atomic force microscopy, Palaeontology, 47(3), 725-743, 10.1111/j.0031-0239.2004.00385.x, 2004.

740 Herfort, L., Thake, B., and Roberts, J.: Acquisition and use of bicarbonate by Emiliania huxleyi, New Phytol, 156(3), 427-436, 10.1046/j.1469-8137.2002.00523.x, 2002.

Hermoso, M.: Coccolith-derived isotopic proxies in palaeoceanography: Where geologists need biologists, Cryptogamie, Algol, 35(4), 323-351, 10.7872/crya.v35.iss4.2014.323, 2014.

Hermoso, M., Horner, T., Minoletti, F., and Rickaby, R.: Constraints on the vital effect in coccolithophore and dinoflagellate

745 calcite by oxygen isotopic modification of seawater, Geochim Cosmochim Ac, 141, 612-627, 10.1016/j.gca.2014.05.002, 2014.

Hermoso, M., Minoletti, F., Aloisi, G., Bonifacie, M., McClelland, H., Labourdette, N., Renforth, P., Chaduteau, C., and Rickaby, R.: An explanation for the 18O excess in Noelaerhabdaceae coccolith calcite, Geochim Cosmochim Ac, 189, 132-142, 10.1016/j.gca.2016.06.016, 2016.

750 Hill, P., Tripati, A., and Schauble, E.: Theoretical constraints on the effects of pH, salinity, and temperature on clumped isotope signatures of dissolved inorganic carbon species and precipitating carbonate minerals, Geochim Cosmochim Ac, 125, 610-652, 10.1016/j.gca.2013.06.018, 2014.

Holtz, L., Wolf-Gladrow, D., and Thoms, S.: Simulating the effects of light intensity and carbonate system composition on particulate organic and inorganic carbon production in Emiliania huxleyi, J Theor Biol, 372, 192-204,

755 10.1016/j.jtbi.2017.01.030, 2015.

Holtz, L., Wolf-Gladrow, D., and Thoms, S.: Stable carbon isotope signals in particulate organic and inorganic carbon of coccolithophores – A numerical model study for Emiliania huxleyi, J Theor Biol, 420, 117-127, 10.1016/j.jtbi.2015.02.024, 2017.

Houdan, A., Probert, I., Zatylny, C., Véron, B., and Billard, C.: Ecology of oceanic coccolithophores. I. Nutritional preferences

760 of the two stages in the life cycle of Coccolithus braarudii and Calcidiscus leptoporus, Aquat Microb Ecol, 44, 291-301, 10.3354/ame044291, 2006.

Hu, B., Radke, J., Schlüter, H., Heine, F., Zhou, L., and Bernasconi, S.: A modified procedure for gas-source isotope ratio mass spectrometry: The long-integration dual-inlet (LIDI) methodology and implications for clumped isotope measurements, Rapid Commun Mass Sp, 28(13), 1413-1425, 10.1002/rcm.6909, 2014.

765 Huntington, K., and Petersen, S.: Frontiers of Carbonate Clumped Isotope Thermometry, Annu Rev Earth Pl Sc, 51, 611-41, 10.1146/annurev-earth-031621, 2023.

Huyghe, D., Daëron, M., de Rafelis, M., Blamart, D., Sébilo, M., Paulet, Y., and Lartaud, F.: Clumped isotopes in modern marine bivalves, Geochim Cosmochim Ac, 316, 41-58, 10.1016/j.gca.2021.09.019, 2022.

Jautzy, J., Savard, M., Dhillon, R., Bernasconi, S., & Smirnoff, A. (2020). Clumped isotope temperature calibration for calcite:

770   Bridging theory and experimentation, Geochem Perspect Lett, 10.7185/geochemlet.2021, 2020.

John, C., and Bowen, D.: Community software for challenging isotope analysis: First applications of 'Easotope' to clumped isotopes, Rapid Commun Mass Sp, 30(21), 2285-2300, 10.1002/rcm.7720, 2016.

Katz, A., Bonifacie, M., Hermoso, M., Cartigny, P., and Calmels, D.: Laboratory-grown coccoliths exhibit no vital effect in clumped isotope (Δ47) composition on a range of geologically relevant temperatures, Geochim Cosmochim Ac, 208, 335-353,

775   10.1016/j.gca.2017.02.025ï, 2017.

Kele, S., Breitenbach, S., Capezzuoli, E., Meckler, A., Ziegler, M., Millan, I., Kluge, T., Deak, J., Hanselmann, K., John, C., Yan, H., Liu, Z., Bernasconi, S.: Temperature dependence of oxygen- and clumped isotope fractionation in carbonates: A study of travertines and tufas in the 6-95°C temperature range, Geochim Cosmochim Ac, 168, 172-192, 10.1016/j.gca.2015.06.032, 2015.

780   Keller, M., Seluin, R., Claus, W., and Guillard, R.: Media for the culture of oceanic ultraphytoplankton, J Phycol, 23, 633-638, https://doi.org/10.1111/j.1529-8817.1987.tb04217.x, 1987.

Kelson, J., Huntington, K., Schauer, A., Saenger, C., and Lechler, A.: Toward a universal carbonate clumped isotope calibration: Diverse synthesis and preparatory methods suggest a single temperature relationship, Geochim Cosmochim Ac, 197, 104-131, 10.1016/j.gca.2016.10.010, 2017.

785   Kester, D., Duedall, I., Connors, D., and Pytkowicz, R.: Preparation of Artificial Seawater, Limnol Oceanogr, 12(1), 176-179, 10.4319/lo.1967.12.1.0176, 1967.

Kim, S. and O'Neil, J.: Equilibrium and nonequilibrium oxygen isotope effects in synthetic carbonates, Geochim Cosmochim Acta, 61(16), 3461–3475, https://doi.org/10.1016/S0016-7037(97)00169-5, 1997.

Langer, G., Geisen, M., Baumann, K-H., Kläs, J., Riebesell, U., Thoms, S., Young, J.R.: Species-specific responses of

790   calcifying algae to changing seawater carbonate chemistry, Geochem Geophy Geosy, 7 (9), 10.1029/2005GC001227, 2006.

Langer, G., Oetjen, K., and Brenneis, T.: Calcification of Calcidiscus leptoporus under nitrogen and phosphorus limitation, J Exp Mar Biol Ecol, 413, 131-137, 10.1016/j.jembe.2011.11.028, 2012.

Lee, K., Kim, T., Byrne, R., Millero, F., Feely, R., and Liu, Y.: The universal ratio of boron to chlorinity for the North Pacific and North Atlantic oceans, Geochim Cosmochim Ac, 74(6), 1801-1811, 10.1038/ncomms13144, 2010.

795   Lee, R., Mavridou, D., Papadakos, G., McClelland, H., and Rickaby, R.: The uronic acid content of coccolith-associated polysaccharides provides insight into coccolithogenesis and past climate, Nature Commun, 7, 10.1016/j.gca.2009.12.027, 2016.

Letulle, T., Gaspard, D., Daëron, M., Arnaud-Godet, F., Vinçon-Laugier, A., Suan, G., and Lécuyer, C.: Multi-proxy assessment of brachiopod shell calcite as a potential archive of seawater temperature and oxygen isotope composition,

800   Biogeosciences, 20(7), 1381-1403, 10.5194/bg-20-1381-2023, 2023.

Leuker, T., Dickson, A., and Keeling, C.: Ocean pCO2 calculated from dissolved inorganic carbon, alkalinity, and equations for K1 and K2: validation based on laboratory measurements of CO2 in gas and seawater at equilibrium, Mar Chem, 70, 105-119, 10.1016/S0304-4203(00)00022-0, 2000.

Leutert, T., Sexton, P., Tripati, A., Piasecki, A., Ho, S., and Meckler, A.: Sensitivity of clumped isotope temperatures in fossil
805   benthic and planktic foraminifera to diagenetic alteration, Geochim Cosmochim Ac, 257, 354-372, 10.1016/j.gca.2019.05.005, 2019.

Levitt, N., Eiler, J., Romanek, C., Beard, B., Xu, H., and Johnson, C.: Near Equilibrium 13C-18O Bonding During Inorganic Calcite Precipitation Under Chemo-Stat Conditions, Geochem Geophy Geosy, 19(3), 901-920, 10.1002/2017GC007089, 2018.

Lewis, E., and Wallace, D.: Program Developed for CO2 System Calculations, 10.15485/1464255, 1998.

810   Matyash, V., Liebisch, G., Kurzchalia, T., Shevchenko, A., and Schwudke, D.: Lipid extraction by methyl-terf-butyl ether for high-throughput lipidomics, J Lipid Res, 49(5), 1137-1146, 10.1194/jlr.D700041-JLR200, 2008.

McClelland, H., Bruggeman, J., Hermoso, M., and Rickaby, R.: The origin of carbon isotope vital effects in coccolith calcite, Nature Commun, 8, 10.1038/ncomms14511, 2017.

McConnaughey, T.: 13C and 18O isotopic disequilibrium in biological carbonates: II. in vitro simulation of kinetic isotope
815   effects, Geochim Cosmochim Ac, 53, 163-171, https://doi.org/10.1016/0016-7037(89)90283-4, 1989.

Meckler, A., Ziegler, M., Millán, M., Breitenbach, S., and Bernasconi, S.: Long-term performance of the Kiel carbonate device with a new correction scheme for clumped isotope measurements, Rapid Commun Mass Sp, 28(15), 1705-1715, 10.1002/rcm.6949, 2014.

Meinicke, N., Ho, S., Hannisdal, B., Nürnberg, D., Tripati, A., Schiebel, R., and Meckler, A.: A robust calibration of the
820   clumped isotopes to temperature relationship for foraminifers, Geochim Cosmochim Ac, 270, 160-183, 10.1016/j.gca.2019.11.022, 2020.

Meinicke, N., Reimi, M., Ravelo, A., Meckler, A.: Coupled Mg/Ca and Clumped Isotope Measurements Indicate Lack of Substantial Mixed Layer Cooling in the Western Pacific Warm Pool During the Last ~5 Million Years. Paleoceanography, e2020PA004115, 10.1029/2020PA004115, 2021.

825   Moolna, A., and Rickaby, R.: Interaction of the coccolithophore Gephyrocapsa oceanica with its carbon environment: Response to a recreated high-CO2 geological past, Geobiology, 10(1), 72-81, 10.1111/j.1472-4669.2011.00308.x, 2012.

Müller, I., Fernandez, A., Radke, J., van Dijk, J., Bowen, D., Schwieters, J., and Bernasconi, S.: Carbonate clumped isotope analyses with the long-integration dual-inlet (LIDI) workflow: scratching at the lower sample weight boundaries, Rapid Commun Mass Sp, 31(12), 1057-1066, 10.1002/rcm.7878, 2017.

830   Müller, I., Rodriguez-Blanco, J., Storck, J., do Nascimento, G., Bontognali, T., Vasconcelos, C., Benning, L., Bernasconi, S.: Calibration of the oxygen and clumped isotope thermometers for (proto-)dolomite based on synthetic and natural carbonates, Chem Geol, 525, 1-17, 10.1016/j.chemgeo.2019.07.014, 2019.

Nimer, N., Guan, Q., and Merrett, M.: Extra- and intra-cellular carbonic anhydrase in relation to culture age in a high-calcifying strain of Emiliania huxleyi Lohmann, New Phytol, 126(4), 601-607, 10.1111/j.1469-8137.1994.tb02954.x, 1994.

835   Peral, M., Daëron, M., Blamart, D., Bassinot, F., Dewilde, F., Smialkowski, N., Isguder, G., Bonnin, J., Jorissen, F., Kissel, C., Michel, E., Vazquez Riveiros, N., Waelbroeck, C.: Updated calibration of the clumped isotope thermometer in planktonic and benthic foraminifera, Geochim Cosmochim Ac, 239, 1-16, 10.1016/j.gca.2018.07.016, 2018.

Peral, M., Bassinot, F., Daëron, M., Blamart, D., Bonnin, J., Jorissen, F., Kissel, C., Michel, E., Waelbroeck, C., Rebaubier, H., Gray, W.: On the combination of the planktonic foraminiferal Mg/Ca, clumped ($\Delta 47$) and conventional ($\delta 18O$) stable
840   isotope paleothermometers in palaeoceanographic studies, Geochim Cosmochim Ac, 339, 22-34, 10.1016/j.gca.2022.10.030, 2022.

Perez, F., and Fraga, F.: Association Constant of Fluoride and Hydrogen ions in seawater, Mar Chem, 21, 168, https://doi.org/10.1016/0304-4203(87)90036-3, 1987.

Phelps, S., Stoll, H., Bolton, C., Beaufort, L., and Polissar, P.: Controls on Alkenone Carbon Isotope Fractionation in the
845   Modern Ocean, Geochem Geophy Geosy, 22(12), 10.1029/2021GC009658, 2021.

Piasecki, A., Bernasconi, S., Grauel, A., Hannisdal, B., Ho, S., Leutert, T., Marchitto, T., Meinicke, N., Tisserand, A., and Meckler, N.: Application of Clumped Isotope Thermometry to Benthic Foraminifera, Geochem Geophy Geosy, 20(4), 2082-2090, 10.1029/2018GC007961, 2019.

Quinn, P., Bowers, R., Zhang, X., Wahlund, T., Fanelli, M., Olszova, D., and Read, B.: cDNA microarrays as a tool for
850   identification of biomineralization proteins in the coccolithophorid Emiliania huxleyi (Haptophyta), Appl Environ Microb, 72(8), 5512-5526, 10.1128/AEM.00343-06, 2006.

Richier, S., Fiorini, S., Kerros, M., von Dassow, P., and Gattuso, J.: Response of the calcifying coccolithophore Emiliania huxleyi to low pH/high pCO2: From physiology to molecular level, Mar Biol, 158(3), 551-560, 10.1007/s00227-010-1580-8, 2011.

855   Rickaby, R., Henderiks, J., and Young, J.: Perturbing phytoplankton: Response and isotopic fractionation with changing carbonate chemistry in two coccolithophore species, Clim Past, 6(6), 771-785, 10.5194/cp-6-771-2010, 2010.

Rost, B., Riebesell, U., Burkhardt, S., and Sültemeyer, D. (2003). Carbon acquisition of bloom-forming marine phytoplankton, Limnol Oceanogr, 48(1), 55-67, 10.4319/lo.2003.48.1.0055, 2003.

Sand, K., Pedersen, C., Sjöberg, S., Nielsen, J., Makovicky, E., and Stipp, S.: Biomineralization: Long-term effectiveness of
860   polysaccharides on the growth and dissolution of calcite, Cryst Growth Des, 14(11), 5486-5494, 10.1021/cg5006743, 2014.

Shackleton, N.: Attainment of isotopic equilibrium between ocean water and the benthonic foraminifera genus Uvigerina: isotopic changes in the ocean during the last glacial, 1974.

Schauble, E., Ghosh, P., and Eiler, J.: Preferential formation of 13C-18O bonds in carbonate minerals, estimated using first-principles lattice dynamics, Geochim Cosmochim Ac, 70(10), 2510-2529, 10.1016/j.gca.2006.02.011, 2006.

865   Schiebel, R., and Hemleben, C.: Planktic foraminifers in the modern ocean, Springer-Verlag Berlin Heidelberg, 366 pp, ISBN 978-3-662-50295-2, 2017.

Sett, S., Bach, L., Schulz, K., Koch-Klavsen, S., Lebrato, M., and Riebesell, U.: Temperature modulates coccolithophorid sensitivity of growth, photosynthesis and calcification to increasing seawater pCO2, PLoS ONE, 9(2), 10.1371/journal.pone.0088308, 2014.

870 Soto, A., Zheng, H., Shoemaker, D., Rodriguez, J., Read, B., and Wahlund, T.: Identification and preliminary characterization of two cDNAs encoding unique carbonic anhydrases from the marine alga Emiliania huxleyi, Appl Environ Microb, 72(8), 5500-5511, 10.1128/AEM.00237-06, 2006.

Spero, H., Bijma, J., Lea, D., Bemis, B.: Effect of seawater carbonate concentration on foraminiferal carbon and oxygen isotopes, Nature, 390, https://doi.org/10.1038/37333, 1997.

875 Spooner, P., Guo, W., Robinson, L., Thiagarajan, N., Hendry, K., Rosenheim, B., and Leng, M.: Clumped isotope composition of cold-water corals: A role for vital effects?, Geochim Cosmochim Ac, 179, 123-141, 10.1016/j.gca.2016.01.023, 2016.

Stevenson, E., Hermoso, M., Rickaby, R., Tyler, J., Minoletti, F., Parkinson, I., Mokadem, F., and Burton, K.: Controls on stable strontium isotope fractionation in coccolithophores with implications for the marine Sr cycle, Geochim Cosmochim Ac, 128, 225-235, 10.1016/j.gca.2013.11.043, 2014.

880 Stoll, H., Ruiz Encinar, J., Ignacio Garcia Alonso, J., Rosenthal, Y., Probert, I., and Klaas, C.: A first look at paleotemperature prospects from Mg in coccolith carbonate: Cleaning techniques and culture measurements, Geochem Geophy Geosy, 2(5), 10.1029/2000GC000144, 2001.

Subhas, A., McCorkle, D., Quizon, A., McNichol, A., and Long, M.: Selective Preservation of Coccolith Calcite in Ontong-Java Plateau Sediments, Paleoceanography and Paleoclimatology, 34(12), 2141-2157, 10.1029/2019PA003731, 2019.

885 Thierstein, H., and Young, J. (Eds.): Coccolithophores, Springer Berlin Heidelberg, 10.1007/978-3-662-06278-4, 2004.

Swart, P., Murray, S., Staudigel, P., Hodell, D.: Oxygen isotopic exchange between CO2 and phosphoric acid: Implications for the measurement of clumped isotopes in carbonates, Geochem Geophys Geosyst, 20(7), 10.1029/2019GC008209, 2019.

Taylor, A., Brownlee, C., Wheeler, G. Coccolithophore Cell Biology: Chalking Up Progress, Annu Rev Mar Sci, 9, 283-310, 10.1146/annurev-marine-122414-034032, 2017.

890 Torres-Romero, I., Clark, A., Wijker, R., Jaggi, M., Zhang, H., Stoll, H.. Temperature-dependent carbon isotope fractionation in coccolithophores, Frontiers in Earth Science, 12, 10.3389/feart.2024.1331179, 2024.

Uchikawa, J., and Zeebe, R.: The effect of carbonic anhydrase on the kinetics and equilibrium of the oxygen isotope exchange in the CO 2-H 2O system: Implications for δ18O vital effects in biogenic carbonates, Geochim Cosmochim Ac, 95, 15-34, 10.1016/j.gca.2012.07.022, 2012.

895 Uchikawa, J., Chen, S., Eiler, J., Adkins, J., and Zeebe, R.: Trajectory and timescale of oxygen and clumped isotope equilibration in the dissolved carbonate system under normal and enzymatically-catalyzed conditions at 25 °C, Geochim Cosmochim Ac, 314, 313-333, 10.1016/j.gca.2021.08.014, 2021.

von Dassow, P., Muñoz Farías, P., Pinon, S., Velasco-Senovilla, E., and Anguita-Salinas, S.: Do Differences in Latitudinal Distributions of Species and Organelle Haplotypes Reflect Thermal Reaction Norms Within the Emiliania/Gephyrocapsa

900 Complex?, Front Mar Sci, 8, 10.3389/fmars.2021.785763, 2021.

Walker, C., Heath, S., Salmon, D., Smirnoff, N., Langer, G., Taylor, A., Brownlee, C., Wheeler, G.. An Extracellular Polysaccharide-Rich Organic Layer Contributes to Organization of the Coccosphere in Coccolithophores, Front Mar Sci, 5(306), 10.3389/fmars.2018.00306, 2018.

Walker, J., Marzec, B., Lee, R., Vodrazkova, K., Day, S., Tang, C., Rickaby, R., Nudelman, F.: Polymorph Selectivity of
905   Coccolith-Associated Polysaccharides from Gephyrocapsa Oceanica on Calcium Carbonate Formation In Vitro, Adv Funct Mater, 29(1), 10.1002/adfm.201807168, 2019.

Watkins, J., and Devriendt, L.: A Combined Model for Kinetic Clumped Isotope Effects in the CaCO3-DIC-H2O System, Geochem Geophy Geosy, 23(8), 10.1029/2021GC010200, 2022.

Watkins, J., and Hunt, J.: A process-based model for non-equilibrium clumped isotope effects in carbonates, Earth Planet Sc
910   Lett, 432, 152-165, 10.1016/j.epsl.2015.09.042, 2015.

Watkins, J., Nielsen, L., Ryerson, F., and DePaolo, D.: The influence of kinetics on the oxygen isotope composition of calcium carbonate, Earth Planet Sci Lett, 375, 349-360, 10.1016/j.epsl.2013.05.054, 2013.

Watkins, J., Hunt, J., Ryerson, F., and DePaolo, D.: The influence of temperature, pH, and growth rate on the δ18O composition of inorganically precipitated calcite, Earth Planet Sci Lett, 404, 332-343, 10.1016/j.epsl.2014.07.036, 2014.

915   Williamson, J.: Least-squares fitting of a straight line, Can J Phys, 18, 1845-1847, 10.1139/p68-523, 1968.

York, D., Evensen, N., Martínez, M., and De Basabe Delgado, J.: Unified equations for the slope, intercept, and standard errors of the best straight line, Am J Phys, 72(3), 367-375, 10.1119/1.1632486, 2004.

Zeebe, R., and Wolf-Gladrow, D.: CO2 in seawater: equilibrium, kinetics, isotopes, Elsevier Oceanography Series, 65, 2001.

Zhang, H., Blanco-Ameijeiras, S., Hopkinson, B., Bernasconi, S., Mejia, L., Liu, C., and Stoll, H.: An isotope label method
920   for empirical detection of carbonic anhydrase in the calcification pathway of the coccolithophore Emiliania huxleyi, Geochim Cosmochim Ac, 292, 78-93, 10.1016/j.gca.2020.09.008, 2021.

Zhang, H., Torres-Romero, I., Anjewierden, P., Jaggi, M., and Stoll, H.: The DIC carbon isotope evolutions during CO2 bubbling: Implications for ocean acidification laboratory culture, Front Mar Sci, 9, 10.3389/fmars.2022.1045634, 2022.

Ziveri, P., Stoll, H., Probert, I., Klaas, C., Geisen, M., Ganssen, G., and Young, J.: Stable isotope 'vital effects' in coccolith
925   calcite, Earth Planet Sci Lett, 210(1-2), 137-149, 10.1016/S0012-821X(03)00101-8, 2003.

Ziveri, P., de Bernardi, B., Baumann, K., Stoll, H., and Mortyn, P.: Sinking of coccolith carbonate and potential contribution to organic carbon ballasting in the deep ocean, Deep-Sea Res Pt II, 54(5-7), 659-675, 10.1016/j.dsr2.2007.01.006, 2007.

Ziveri, P., Thoms, S., Probert, I., Geisen, M., and Langer, G.: A universal carbonate ion effect on stable oxygen isotope ratios in unicellular planktonic calcifying organisms, Biogeosciences, 9(3), 1025-1032, 10.5194/bg-9-1025-2012, 2012.

930   **Tables**

Species	Temperature (°C)	Final CO$_{2(aq)}$ (μM)	Culture setup type	Δ^{13}C$_{c-DIC}$ (‰ V-PDB ± 1σ)	Δ^{18}O$_{c-sw}$ (‰ V-SMOW ± 1σ)	Δ$_{47}$ (‰ I-CDES ± 1SE)

G. oceanica	12	14.66	Batch	-0.40 ± 0.47	32.95 ± 0.34	0.640 ± 0.009
	15	21.56	Continuous	-0.87 ± 1.12	31.29 ± 0.26	0.621 ± 0.009
	15	33.01	Continuous	0.03 ± 0.18	31.57 ± 0.25	0.634 ± 0.008
	15	40.18	Continuous	-0.24 ± 0.13	31.68 ± 0.26	0.637 ± 0.013
	18	6.94	Continuous	-1.15 ± 0.69	31.37 ± 0.13	0.628 ± 0.009
	18	7.95	Continuous	-1.41 ± 0.70	31.03 ± 0.26	0.629 ± 0.005
	18	18.41	Continuous	0.54 ± 1.00	30.65 ± 0.15	0.620 ± 0.004
	18	24.12	Continuous	-0.95 ± 1.00	30.74 ±0.13	0.620 ± 0.010
	18	27.73	Continuous	0.51 ± 1.00	30.63 ± 0.12	0.629 ± 0.008
	18	42.58	Continuous	-0.78 ± 0.35	30.45 ± 0.11	0.633 ± 0.005
	21	5.62	Continuous	-0.24 ± 0.25	30.45 ± 0.14	0.624 ± 0.007
	21	6.18	Continuous	0.75 ± 0.25	30.47 ± 0.17	0.611 ± 0.008
	21	6.18	Continuous	0.69 ± 0.27	30.37 ± 0.22	0.626 ± 0.004
	21	7.63	Continuous	-0.61 ± 0.25	30.44 ± 0.35	0.621 ± 0.005
	21	11.68	Continuous	-0.38 ± 0.15	30.15 ± 0.11	0.618 ± 0.012
	21	12.83	Continuous	-0.43 ± 0.13	30.26 ± 0.07	0.608 ± 0.012
	21	21.23	Continuous	1.22 ± 1.05	30.77 ± 0.33	0.620 ± 0.005
	21	21.23	Continuous	1.22 ± 1.05	30.76 ± 0.33	0.604 ± 0.008
	21	29.48	Continuous	-0.49 ± 0.32	30.74 ± 0.86	0.630 ± 0.007
	21	30.76	Continuous	-0.66 ± 0.32	30.92 ± 0.86	0.625 ± 0.011
	21	43.22	Continuous	-1.21 ± 1.05	30.57 ± 0.34	0.603 ± 0.004
	21	43.22	Continuous	-1.25 ± 1.05	30.56 ± 0.33	0.607 ± 0.006
	21	43.76	Continuous	-0.98 ± 1.05	30.45 ± 0.33	0.611 ± 0.010
	24	13.05	Continuous	0.78 ± 0.34	29.39 ± 0.09	0.599 ± 0.005
	24	13.05	Continuous	0.85 ± 0.34	29.44 ± 0.10	0.598 ± 0.008
	24	13.73	Batch	-0.80 ± 0.28	29.09 ± 0.41	0.605 ± 0.007
	24	14.07	Batch	-0.21 ± 0.28	29.70 ± 0.37	0.611 ± 0.008
	24	16.95	Continuous	0.65 ± 0.34	29.72 ± 0.10	0.607 ± 0.010
	24	19.18	Continuous	-0.87 ± 0.39	29.38 ± 0.14	0.589 ± 0.006
	27	15.11	Continuous	0.61 ± 0.82	29.10 ± 0.13	0.603 ± 0.007
	27	15.11	Continuous	0.61 ± 0.82	29.03 ± 0.11	0.597 ± 0.007
G. muellerae	6	14.40	Batch	-0.88 ± 0.03	33.90 ± 0.28	0.659 ± 0.006
	6	14.57	Batch	-0.57 ± 0.03	34.00 ± 0.28	0.655 ± 0.005
	12	16.34	Batch	0.03 ± 0.21	32.48 ± 0.71	0.648 ± 0.005
	12	21.22	Batch	0.21 ± 0.21	32.98 ± 0.70	0.645 ± 0.008
	18	7.94	Batch	-0.88 ± 0.35	31.28 ± 0.24	0.618 ± 0.010
	18	9.80	Batch	-0.26 ± 0.35	31.31 ± 0.24	0.629 ± 0.009
C. leptoporus	12	17.94	Batch	-2.34 ± 0.42	29.78 ± 0.36	0.645 ± 0.006
	12	17.94	Batch	-2.22 ± 0.42	29.93 ± 0.35	0.652 ± 0.005
	12	19.12	Batch	-2.86 ± 0.49	29.89 ± 0.57	0.636 ± 0.008

Table 1. Overview table for all included data points for Sect. 3, 4.1, 4.2. including temperature (°C), culture setup type, $CO_{2(aq)}$ (µM), $\Delta^{13}C_{c\text{-DIC}}$ (‰; VPDB), $\Delta^{18}O_{c\text{-sw}}$ (‰; VSMOW), and Δ_{47} values (‰; I-CDES). 1 standard deviation (σ) is included for the $\Delta^{13}C_{c\text{-DIC}}$ and $\Delta^{18}O_{c\text{-sw}}$, which take the evolution of the media over time into account, and 1 standard error (SE) for Δ_{47}.

Data type	Slope	Intercept
G. oceanica	0.0377 ± 0.009	0.179 ± 0.104
G. oceanica + G. muellerae	0.0360 ± 0.005	0.198 ± 0.063
G. oceanica + C. leptoporus	0.0387 ± 0.007	0.168 ± 0.083
Temperature-weighted averages	0.0358 ± 0.006	0.202 ± 0.073
All species	0.0367 ± 0.005	0.190 ± 0.059
Including excluded data	0.0375 ± 0.004	0.181 ± 0.048

935 **Table 2. Slope and intercepts with 1σ for the Δ_{47}-temperature regression using the Williamson-York bivariate least-squares method.**

	pH	DIC	$CO_{2(aq)}$	$\Delta^{13}C_{C\text{-DIC}}$	$\Delta\Delta^{18}O_{off}$
All measured $\Delta\Delta_{47,off}$	0.17	-0.01	-0.09	0.04	0.08
Continuous setup $\Delta\Delta_{47,off}$	0.27	-0.04	-0.13	0.09	0.45*
Batch setup $\Delta\Delta_{47,off}$	-0.32	0.20	0.11	0.13	-0.19

Table 3. Pearson correlation coefficients (ρ) between $\Delta\Delta_{47,off}$ and pH, DIC, and $CO_{2(aq)}$ for all measurements, continuous culture, and batch culture setup. Asterisk indicates where p-value is < 0.05.

	Measured Δ_{47} in this study	Peral et al. (2018; 2022)	Meinicke et al. (2020; 2021)	Daëron and Vermeesch (2024) MIT	Daëron and Gray (2023) orig	Daëron and Gray (2023) recal
Method of temperature measurement or estimation	Experimental measurements	Empirical estimated $\delta^{18}O$-T calibration of Kim and O'Neil (1997)	Empirical estimated $\delta^{18}O$-T calibration of Shackleton (1974)	Experimental and natural inorganic calcite measurements	Empirical estimated $\delta^{18}O$-T calibration of Shackleton (1974) and Kim and O'Neil (1997)	Recalculated using empirical estimated $\delta^{18}O$-T calibration of Kim and O'Neil (1997) and species specific $\delta^{18}O$ fractionations
$\Delta\Delta_{47,off}$ residuals (ppm ± 1σ)	-0.6 ± 3.4	-3.2 ± 0.2	-3.1 ± 1.3	-7.9 ± 0.5	-5.7 ± 0.7	-8.5 ± 0.6
Temperature offset (°C ± 1σ)	0.19 ± 1.12	-1.03 ± 0.02	-0.99 ± 0.36	-2.56 ± 0.05	-1.86 ± 0.35	-2.77 ± 0.39

940 **Table 4. Average $\Delta\Delta_{47,off}$ residuals relative to our dataset comparing our coccolith calibration equations and those from the Peral et al. (2018; 2022), Meinicke et al. (2020; 2021), Daëron and Vermeesch (2024) MIT, Daëron and Gray (2023) original temperatures,**

and Daëron and Gray (2023) recalculated temperatures. Equivalent temperature offset is based on the equivalent Δ_{47} value at the average growth temperature (18.7°C) using Equation 4. Method of measurement or estimation of temperatures for each study is given.

945 **Figures**
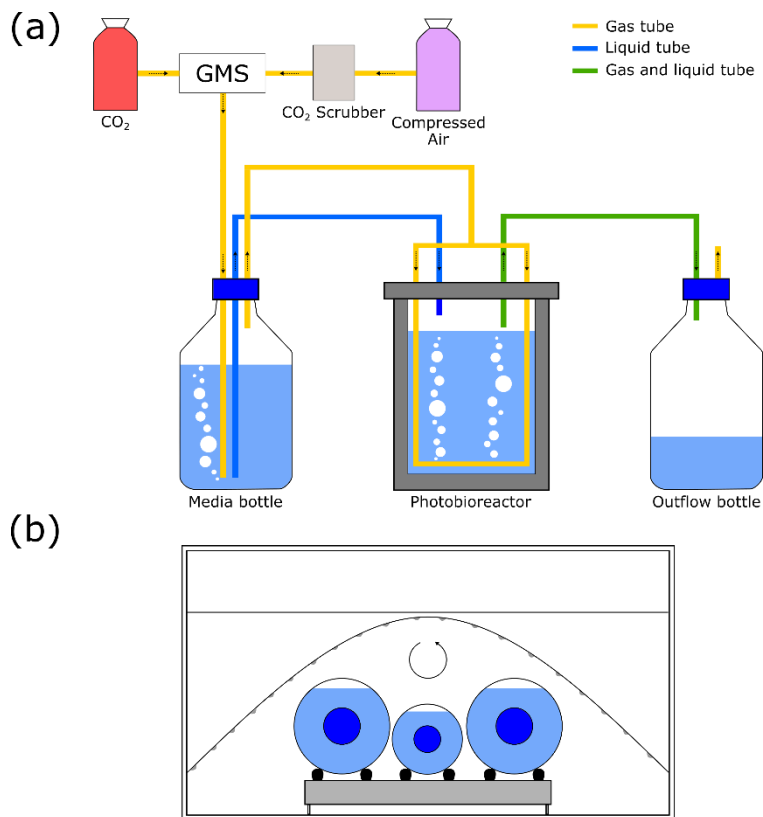
Figure 1. Photobioreactor and incubator systems. (a) Photobioreactor with controlled CO_2 gas input, adjusted from Zhang et al. (2022), (b) Incubator with roller containing 2 2L and 1 1L bottle and LED strip for batch cultures.
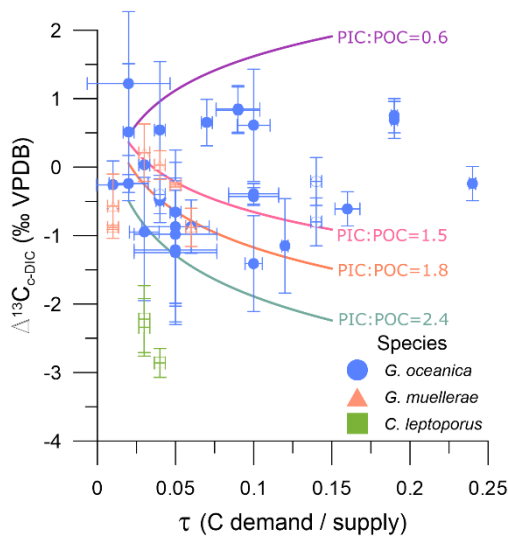
950

Figure 2. Coccolith carbon isotope fractionation relative to external DIC (Δ¹³C$_{c\text{-DIC}}$) against the carbon demand vs supply (τ). Blue circles are *G. oceanica*, orange triangles are *G. muellerae*, and green squares are *C. leptoporus*. Open and filled symbols are batch and continuous cultures respectively. Error bars are as described in methods. Lines represent the model simulations of McClelland et al. (2017) at different PIC:POC ratios; purple = 0.6, pink = 1.5, orange = 1.8, grey = 2.4.

955
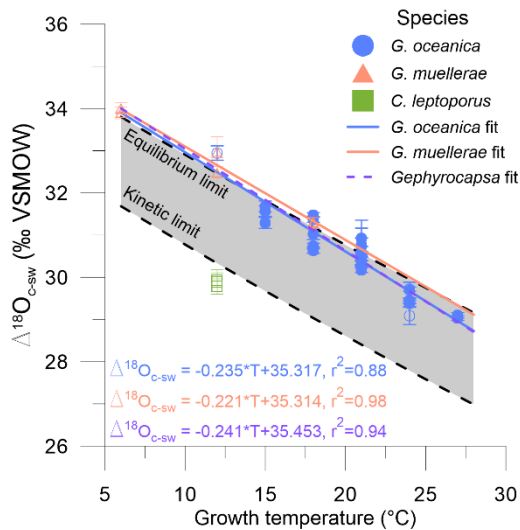
Figure 3. The fractionation of oxygen isotopes in coccolith calcite from seawater (Δ¹⁸O$_{c\text{-sw}}$), both in VSMOW, in relation to the growth temperature in °C. Blue circles are *G. oceanica*, orange triangles are *G. muellerae*, and green squares are *C. leptoporus*. Open and filled symbols are batch and continuous cultures respectively. Linear regression fits are calculated for *G. oceanica* and *G.
960 ***muellerae* separately, as well as for the whole *Gephyrocapsa* genus, with equivalent formulae. Error bars are as described in methods, temperature error bars are smaller than symbols. The ~~kinetic and~~ equilibrium and kinetic limits are from Watkins et al. (2014) and defined as $\left(\frac{17747}{T+273.15}\right) - 29.77$ and $\left(\frac{17965}{T+273.15}\right) - 32.67$ respectively.**
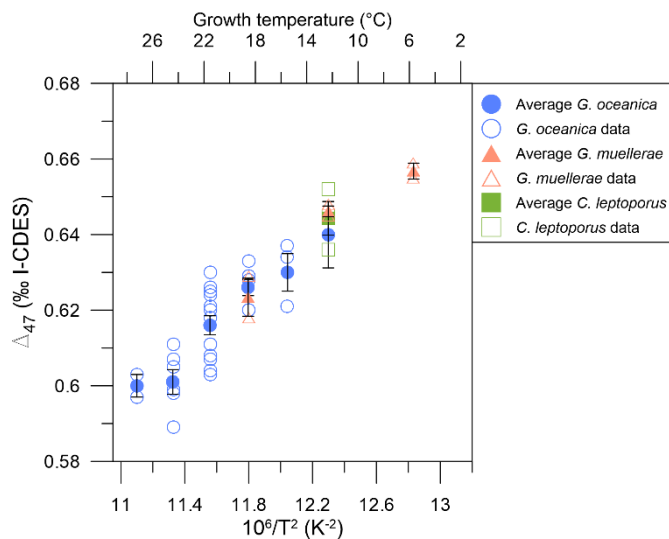
965 **Figure 4. Δ_{47} values from coccolith calcite versus $10^6/T^2$ for all data points and averages. Averages are full symbols, while individual datapoints are empty symbols. Blue circles are *G. oceanica*, orange triangles are *G. muellerae*, and green squares are *C. leptoporus* data. Error bars are as described in methods, temperature error bars are smaller than symbols.**
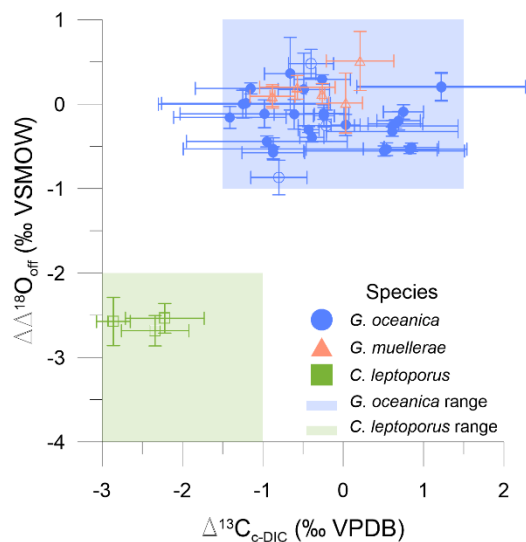
970 **Figure 5. The oxygen isotope offset from the equilibrium limit in Watkins et al., (2014) ($\Delta\Delta^{18}O_{off}$) against the coccolith carbon isotope fractionation relative to external DIC ($\Delta^{13}C_{c-DIC}$). Blue circles are *G. oceanica*, orange triangles are *G. muellerae*, and green squares are *C. leptoporus* data. Open and filled symbols are batch and continuous cultures respectively. The $\Delta^{13}C_{c-DIC}$ and $\Delta\Delta^{18}O_{off}$ range of previous *G. oceanica* and *C. leptoporus* studies are given as a blue and green background respectively. Error bars are as described in methods.**

975
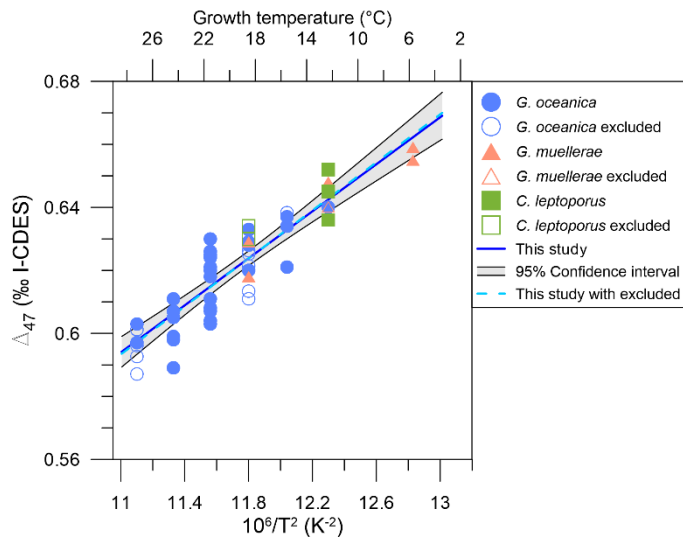
Figure 6. Δ47 values compared to temperature (in K) for cultured coccoliths. York regression and its 95% confidence interval are shown as a blue line and light grey envelope. The species are colour and symbol coded following Fig. 2. Blue circles are *G. oceanica*, orange triangles are *G. muellerae*, and green triangles are *C. leptoporus*. Empty symbols are excluded data but still included for illustration and the coccolith Δ47-temperature calibration.
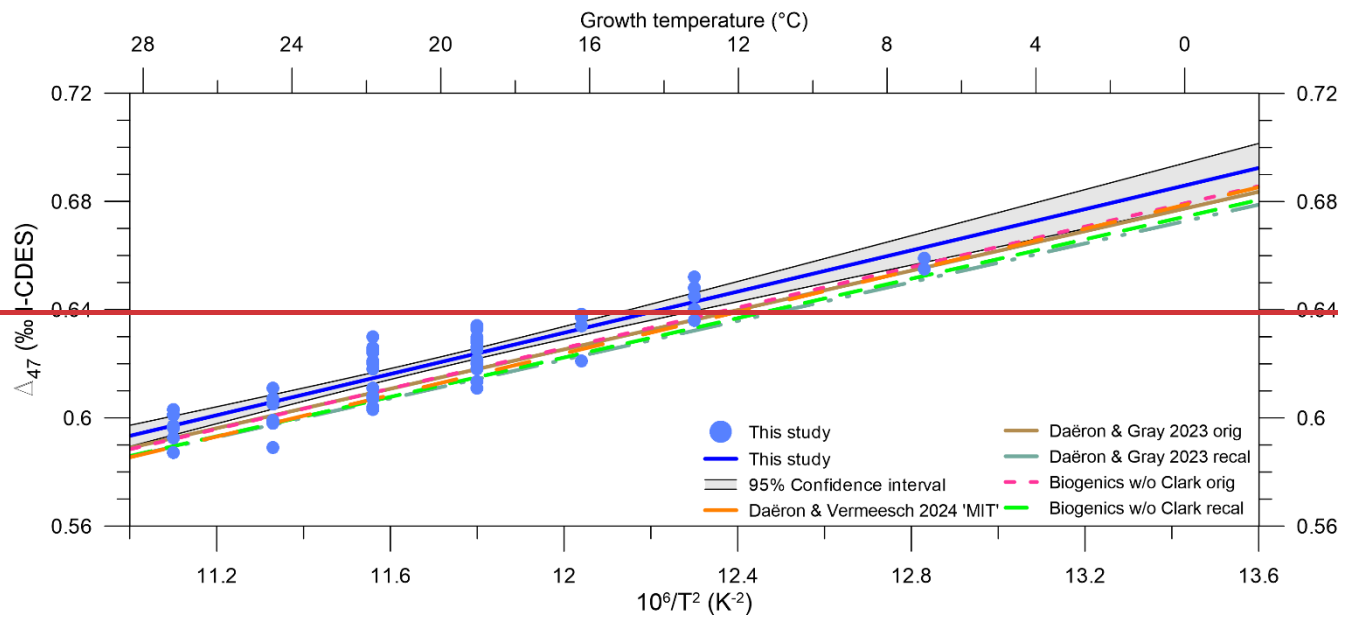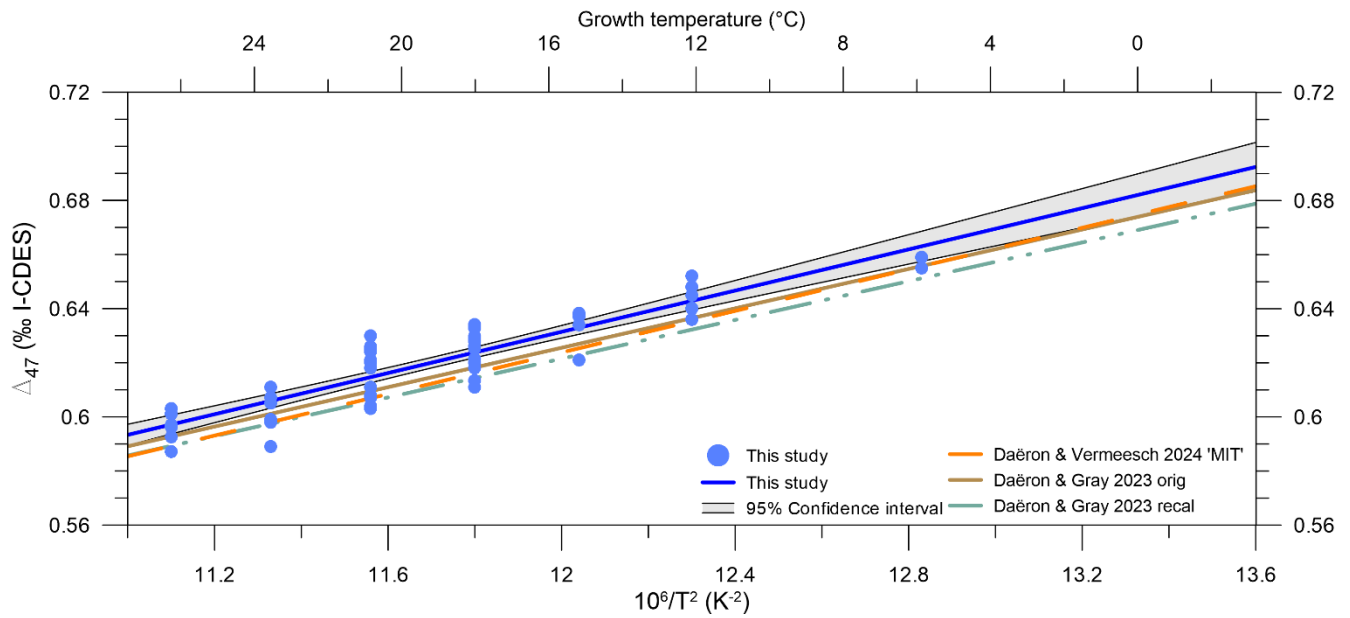
Figure 7. Δ_{47} versus temperature for coccolith calcite and previous biogenic and inorganic calibrations. The York linear fit and 95%
confidence interval for the unified coccolith calcite Δ_{47}-temperature is shown as a blue line with grey shading. Daëron and Gray
(2023 orig; brown dash-dot dot-dash line), Daëron and Gray (2023 recal; grey dash-dot dot-dash line), and Daëron and Vermeesch
(2024 'MIT'; orange ~~dashed line), biogenic calibration without this study using original published temperatures (pink dashed line),~~
~~and biogenic calibration without this study using recalculated temperatures (green~~ **dashed line).**

985
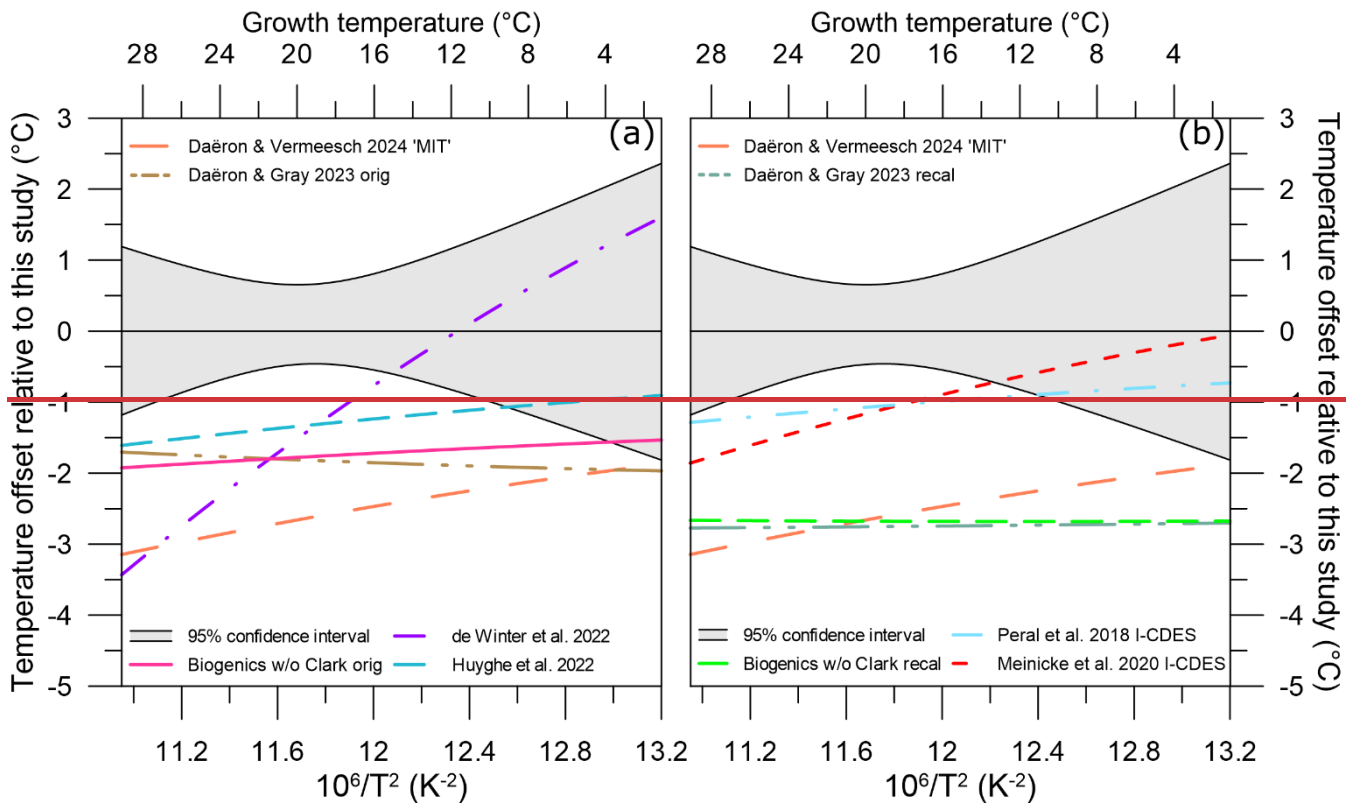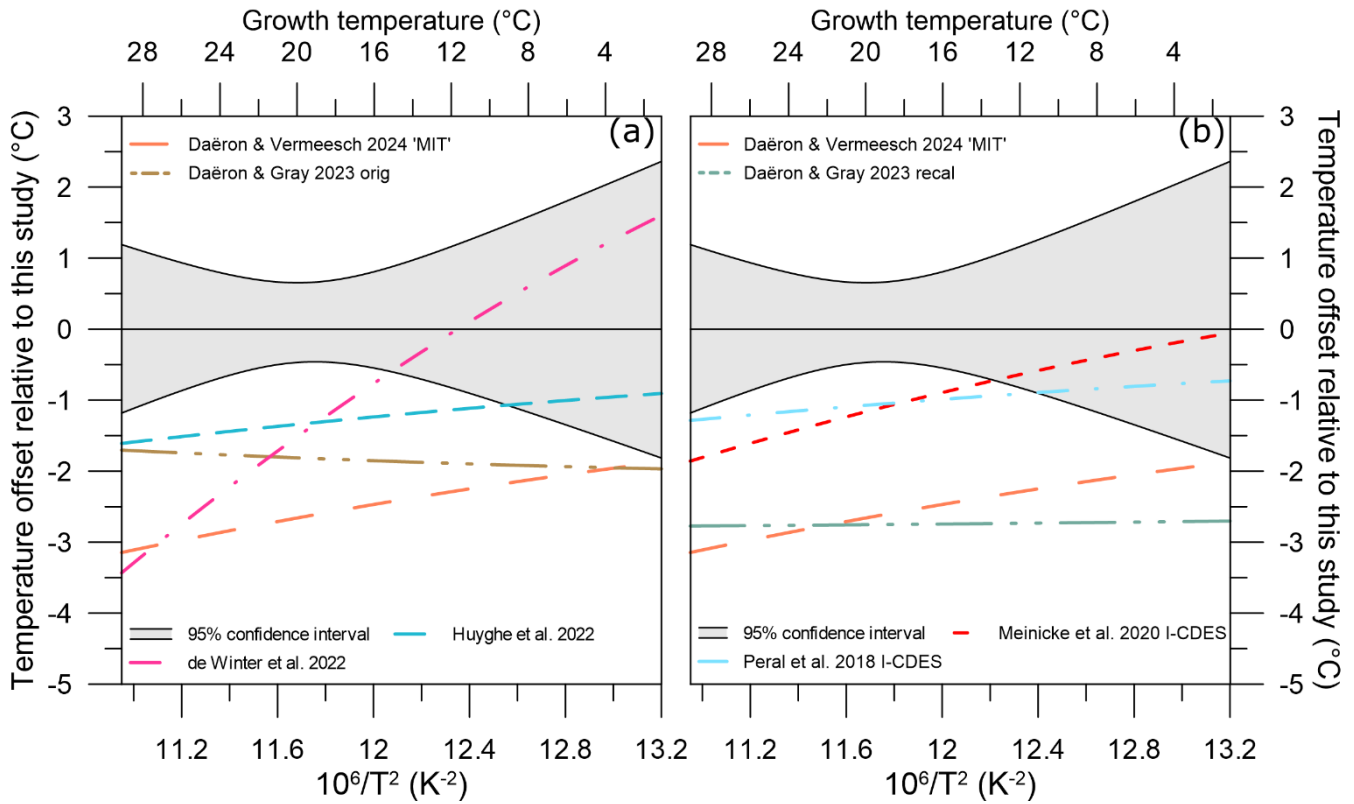
Figure 8. Temperature offset of different Δ₄₇-temperature calibrations relative to our study's equivalent temperature. ~~The other studies'~~ a) Temperature offsets of two non-foraminifera biogenic carbonate calibration ~~data are colour coded following Fig. 7, with additional~~ studies ~~of Peral et al. ; (2018; light blue dash-dot-dash line) and Meinicke et al. (2020; red dashed line),~~ de Winter et al. (2022; ~~purple~~pink dash-dot-dash line~~),~~) and Huyghe et al. (2022; blue dashed line). b) Temperature offsets of two planktic foraminifera biogenic carbonate calibration studies; Peral et al. (2018; light blue dash-dot-dash line) and Meinicke et al.)(2020; red dashed line), using original published temperatures. Other included studies' calibration data are colour coded following Fig. 7. The 95% confidence interval for our study is given as light grey shading.